Comparison of FRPE and Human Embryonic Stem Cell–Derived RPE Behavior on Aged Human Bruch's Membrane

Ilene K. Sugino,[1] Qian Sun,[1] Jianqiu Wang,[1] Celia F. Nunes,[1] Noounanong Cheewatrakoolpong,[1] Aprille Rapista,[1] Adam C. Johnson,[1] Christopher Malcuit,[2,3] Irina Klimanskaya,[2] Robert Lanza,[2] and Marco A. Zarbin[1]

Purpose. To compare RPE derived from human embryonic stem cells (hES-RPE) and fetal RPE (fRPE) behavior on human Bruch's membrane (BM) from aged and AMD donors.

Methods. hES-RPE of 3 degrees of pigmentation and fRPE were cultured on BM explants. Explants were assessed by light, confocal, and scanning electron microscopy. Integrin mRNA levels were determined by real-time polymerase chain reaction studies. Secreted proteins in media were analyzed by multiplex protein analysis after 48-hour exposure at culture day 21.

Results. hES-RPE showed impaired initial attachment compared to fRPE; pigmented hES-RPE showed nuclear densities similar to fRPE at day 21. At days 3 and 7, hES-RPE resurfaced BM to a limited degree, showed little proliferation (Ki-67), and partial retention of RPE markers (MITF, cytokeratin, and CRALBP). TUNEL-positive nuclei were abundant at day 3. fRPE exhibited substantial BM resurfacing at day 3 with decreased resurfacing at later times. Most fRPE retained RPE markers. Ki-67–positive nuclei decreased with time in culture. TUNEL staining was variable. Increased integrin mRNA expression did not appear to affect cell survival at day 21. hES-RPE and fRPE protein secretion was similar on equatorial BM except for higher levels of nerve growth factor and thrombospondin-2 (TSP2) by hES-RPE. On submacular BM, fRPE secreted more vascular endothelial growth factor (VEGF), brain-derived neurotrophic factor, and platelet-derived growth factor; hES-RPE secreted more TSP2.

Conclusions. Although pigmented hES-RPE and fRPE resurfaced aged and AMD BM to a similar, limited degree at day 21, cell behavior at earlier times was markedly dissimilar. Differences in protein secretion may indicate that hES-RPE may not function identically to native RPE after seeding on aged or AMD BM. (*Invest Ophthalmol Vis Sci.* 2011;52:4979–4997) DOI: 10.1167/iovs.10-5386

Cell-based therapy involving RPE transplantation might preserve or restore vision in AMD patients with evolving atrophy or in patients with other diseases in which vision loss is associated with dysfunctional RPE. Cell transplantation in patients with AMD has been attempted using a number of cell types and preparations, including fetal and adult RPE (autologous and allogeneic), translocated autologous choroid/RPE, and autologous iris pigment epithelium (IPE; see review by Binder[1]). Transplantation of autologous RPE and IPE is attractive because there is no risk of immune rejection. However, older cells: (1) do not behave as robustly as those from young donors,[2–4] (2) may carry AMD-related gene defects or modifications caused by aging,[1,5,6] and (3) may not have the ability to perform all the functions necessary to maintain the photoreceptors.[5] Because fetal human RPE begin to show morphologic abnormalities after five to six passages, they are not suitable as a "universal" donor source, regardless of the possible immunogenicity of such cells.[7] In addition, the supply of RPE from young donors is limited, so it would not be practical to develop a RPE transplant paradigm based on the use of such cells. Embryonic stem cells offer an advantage over fetal or adult RPE because of their ability to undergo large-scale expansion, assuring an abundant supply of well characterized, pathogen-free cells that can be manufactured in a manner compatible with clinical practice.[8] Genetic analysis of such cells shows a high degree of similarity to in situ RPE.[9] The method to generate RPE derived from human embryonic stem cells (hES-RPE) is reproducible and can be achieved in a manner that does not cause embryo destruction.[10] Manipulation of hES-RPE in culture could take advantage of stem cell plasticity to optimize their ability to attach and survive on aged or diseased Bruch's membrane (BM) and to minimize rejection.[11] To assess the potential of hES-RPE for cell replacement therapy in AMD patients, we compared the attachment and survival of hES-RPE of different degrees of pigmentation on BM with cultured human fetal RPE (fRPE) whose behavior has been characterized

From the [1]The Institute of Ophthalmology and Visual Science, New Jersey Medical School, University of Medicine and Dentistry of New Jersey, Newark, New Jersey; and [2]Advanced Cell Technology Inc., Worcester, Massachusetts.

[3]Present affiliation: Bioengineering Institute, Worcester Polytechnic Institute, Worcester, Massachusetts.

Supported in part by the Foundation Fighting Blindness, the Lincy Foundation, an unrestricted grant from Research to Prevent Blindness, The Eye Institute of New Jersey, the Janice Mitchell Vassar and Ashby John Mitchell Fellowship, the Joseph J. and Marguerite DiSepio Retina Research Fund, the Foundation of UMDNJ, and the New Jersey Lions Eye Research Foundation. Provision of fetal donor eyes from the University of Washington Laboratory of Developmental Biology was supported by National Institutes of Health R24HD000836 (Ian Glass, PI). The content does not necessarily represent the official views of the Eunice Kennedy Shriver National Institute of Child Health and Human Development of the National Institutes of Health.

Submitted for publication February 17, 2010; revised June 27, 2010 and February 9, 2011; accepted March 8, 2011.

Disclosure: **I.K. Sugino**, Advanced Cell Technology (F); **Q. Sun**, Advanced Cell Technology (F); **J. Wang**, Advanced Cell Technology (F); **C.F. Nunes**, Advanced Cell Technology (F); **N. Cheewatrakoolpong**, Advanced Cell Technology (F); **A. Rapista**, Advanced Cell Technology (F); **A.C. Johnson**, Advanced Cell Technology (F); **C. Malcuit**, Advanced Cell Technology (E); **I. Klimanskaya**, Advanced Cell Technology (E); **R. Lanza**, Advanced Cell Technology (E); **M.A. Zarbin**, Advanced Cell Technology (C, F)

Corresponding author: Marco A. Zarbin, Professor and Chair, Institute of Ophthalmology and Visual Science, University of Medicine and Dentistry of New Jersey, 90 Bergen Street, DOC 6155, Newark, NJ 07101; zarbin@umdnj.edu.

previously on aged and AMD BM.[4,12,13] The goals of this study were to determine: (1) whether hES-RPE have the potential to attach and survive on aged BM; (2) whether a characteristic integrin mRNA profile can predict attachment and/or survival; (3) whether hES-RPE and fRPE have similar morphology after attachment to and growth on BM; and (4) whether hES-RPE secrete neurotrophic proteins after attachment and survival on aged human BM.

Using the same hES-RPE preparations as in the present study, Lu et al.[8] demonstrated long-term safety and functionality of hES-RPE after subretinal injection in rodents. These and other studies using hES-RPE derived in a similar fashion from spontaneously forming pigmented colonies in confluent hES cultures have shown that hES-RPE express RPE-specific genes, phagocytose outer segments, show polarization of Na^+/K^+ ATPase, and exhibit morphologic features of RPE.[8,9,14–16] Therefore, hES-RPE might serve well for RPE replacement therapy in patients with retinal degenerations where the primary cause of vision loss is diseased or missing RPE. Although animal studies show that hES-RPE can survive in the subretinal space and rescue photoreceptors,[8,14,16,17] such studies do not always predict the ability of cells to survive on diseased BM in AMD patients.[18]

Integrins are important for RPE attachment to BM (reviewed by Afshari[19]), and alpha integrin subunits have an important role in RPE adhesion to this surface.[20] In cultured cells, integrin expression can be modulated by the degree of and time at confluence,[21] and integrin upregulation through culturing improves RPE and iris pigment epithelium (IPE) adhesion to BM.[4,20,22] One criterion by which one might assess hES-RPE as candidates for transplantation in AMD eyes is the presence of an integrin mRNA profile compatible with attachment to BM (e.g., a profile similar to that of cultured fRPE), which show robust attachment to BM by 24 hours after seeding.[4,12,20] To determine whether the integrin mRNA profile can predict successful hES-RPE adhesion and survival on aged submacular human BM, we compared integrin mRNA expression and survival on BM of three different batches of hES-RPE of different degrees of pigmentation (harvested at increasing times in culture) with that of fRPE.

In addition to replacing lost or diseased RPE cells with cells capable of performing RPE functions, transplanted cells could rescue dying photoreceptors through the secretion of proteins such as neurotrophic factors and cytokines. This idea is supported by in vivo studies showing that non-RPE cells can rescue photoreceptors despite their inability to phagocytose outer segments.[23–26] Therefore, even if the cells do not appear to be fully differentiated on BM after transplantation, secretion of neuroprotective growth factors might have a rescue effect on the overlying retina. As a result, in the studies reported here, we also compared growth factor and cytokine secretion into the media overlying BM explants on which hES-RPE and fRPE were seeded.

Material and Methods

Studies involving use of human donor tissue followed the tenets of the Declaration of Helsinki and were approved by the institutional review board of the University of Medicine and Dentistry of New Jersey.

Generation of hES-RPE

The following procedures were performed at facilities located at Advanced Cell Technology (ACT; Worcester, MA). (Please see Lu et al.[8] for details on safety and efficacy studies performed on these cells.)

hES-RPE were obtained from a single blastomere-derived human embryonic stem cell line designated MA01 using private funds at ACT.[10,27] Human embryonic stem cells (hESCs) were co-cultured on mitotically inactivated primary mouse embryonic fibroblasts (ICR; Taconic Farms, Germantown, NY) as previously described.[28] Once cultures were near confluence, hESCs were dissociated by trypsinization (0.05% trypsin/0.53mM EDTA; Invitrogen, Carlsbad, CA) and mechanically dispersed with an 18-gauge needle. Single-cell suspensions were then cultured in low attachment plates (Corning Costar; Lowell, MA) to allow for embryoid body formation for seven to 10 days in MDBK-GM (Sigma-Aldrich; St. Louis, MO) supplemented with 1X B-27 supplement (Gibco, Life Technologies, Carlsbad, CA) (differentiation medium). Embryoid bodies were then plated onto 0.1% gelatin-coated dishes (STEMCELL Technologies; Vancouver, BC) at a 1:1 to 1:2 split ratio in the same medium. After 3 weeks of culture, clusters of differentiated hES-RPE cells were separated by 3-hour exposure to type IV collagenase (4 mg/mL; Invitrogen, Life Technologies) followed by mechanical separation from nonpigmented cells.[9] Isolated hES-RPE clusters were then dissociated by 10-minute incubation in a 1:1 mixture of 0.25% trypsin/1 mM EDTA and Hank's-based cell dissociation buffer (both from Invitrogen, Life Technologies). Cells were then pelleted by centrifugation, resuspended in EGM-2 (RPE expansion medium; Lonza Biologics, Allendale, NJ), and plated onto gelatin-coated dishes. Isolated hES-RPE were grown continuously on gelatin-coated dishes in RPE expansion medium and subcultured twice at a 1:3 split ratio. After the second passage post-isolation, hES-RPE were maintained in the same culture vessels in hES-RPE expansion medium for approximately 7 days, at which point cells displayed little to no detectable pigmentation with a fibroblastic morphology. Cells harvested at this point were dubbed "hES-RPE1" (total culture time from isolation, 6 weeks). The remaining cultures were changed to RPE maintenance medium (MDBK-MM; Sigma-Aldrich), allowed to grow to confluence, and began to regain typical RPE cell morphology of a cobblestone-like appearance with accumulated pigmentation. During this time, cells were harvested at two additional arbitrary time points when cells displayed the following morphologies: hES-RPE2, harvested when the cells gained epithelioid morphology with greater than half of the cell population possessing accumulated pigmentation, was achieved by culturing for an approximately 3 additional weeks (total culture time from isolation, approximately 9 weeks); hES-RPE3, similar in morphology to hES-RPE2 but with greater than 85% of the cell population possessing accumulated pigmentation, was achieved by culturing for an additional 4 to 5 weeks (total culture time from isolation, approximately 10–11 weeks). (See Fig. 1 in Lu et al.[8] for pictures of hES-RPE cultures.) All batches were cryopreserved in a cryoprotectant medium containing fetal bovine serum (Hyclone; Thermo Fisher Scientific, Waltham, MA) and 10% DMSO (Sigma-Aldrich) and stored in the vapor phase above liquid nitrogen. Cell viability after thaw before seeding on BM was determined by trypan blue staining.

fRPE Isolation and Culture

Human fRPE are robust cells that can attach, resurface, and survive on aged BM to some degree.[4,12,13,29] For each study, the behavior of hES-RPE and cultured fRPE was compared on paired submacular BM specimens from a single donor. All fRPE cultures used in this study were from fresh cultures (i.e., cultures that were not established from frozen stock) to eliminate freeze/thaw effects on the viability and robustness of the cells. fRPE cultures were established from donor eyes (9 donors, 16–21 gestational weeks) obtained from Advance Bioscience Resources, Inc. (Alameda, CA) and the Laboratory of Developmental Biology (University of Washington, Seattle, WA). Sheets of fRPE were isolated from RPE/choroid pieces after incubation in 0.8 mg/mL collagenase type IV (Sigma-Aldrich) as previously described.[4] Cells were seeded and passaged onto bovine corneal endothelial cell-extracellular matrix (BCE-ECM)–coated tissue culture dishes prepared in this laboratory according to a previously described protocol.[30] Primary cultures were checked routinely for choroidal cell contamination (using morphologic criteria) before passage to assure purity of the cultures. After achieving confluence, primary cultures were passaged at a 1:6 split ratio onto BCE-ECM–coated dishes using 0.25% trypsin-EDTA

(Gibco, Life Technologies) to harvest the cells. Subsequent cultures were passaged at a 1:4 split ratio. RPE were cultured in "RPE media" comprising DMEM (Cellgro, Mediatech, Inc., Manassas, VA) supplemented with 15% fetal bovine serum (Hyclone, Thermo Fisher Scientific), 2.5 μg/mL amphotericin B (Gibco, Life Technologies), 2 mM L-glutamine (Gibco, Life Technologies), 50 μg/mL gentamicin (Cellgro, Mediatech), and 1 ng/mL basic fibroblast growth factor (Invitrogen, Life Technologies) at 37°C in 10% CO_2. Cells of passage one through four 3 to 9 days after seeding onto culture dishes, were harvested for seeding onto BM.

Organ Culture Assay

Human donor eyes (23 donors; mean age, 74.35± 7.11 years) were received through the National Disease Resource Interchange (Philadelphia, PA), the Midwest Eyebanks (Ann Arbor, MI), and the Lions Eye Institute for Transplant and Research, Inc. (Tampa, FL). Acceptance criteria included: age 55 years or older, no recent history of chemotherapy or radiation to the head, no ventilatory support before death, no head trauma, no ocular history affecting the posterior segment, enucleation within 7 hours postmortem, and receipt within 48 hours from time of death. Submacular pathology was noted by visual examination of the posterior pole with a dissecting microscope (Stemi SV11; Carl Zeiss, Inc., Thornwood, NY) after removal of the retina and by light microscopic analysis of sectioned BM-choroid-sclera explants (termed "BM explants") (see Methods, Light microscopic explant analysis). All eyes used in this study were from Caucasian donors. Donor information is included in Table 1.

BM explants were prepared as described previously using mechanical RPE debridement. For submacular debridement, a moist surgical sponge (Alcon, Fort Worth, TX) was used to expose the superficial inner collagenous layer (ICL).[13] A wedge-shaped brush obtained from a local artist supply store was used for equatorial RPE debridement. (Attachment on the ICL was studied because this surface will likely be encountered in cell transplantation after choroidal new vessel re-

Table 1. Human Donor Eye Information and Resulting Nuclear Density of Human Embryonic Stem Cell–derived RPE or Fetal RPE on Submacular Bruch's Membrane Explants 21 Days After Seeding

Age (y)	D to P	D to R	COD	Submacular Pathology hES-RPE Explant	Submacular Pathology fRPE Explant	hES-RPE ND ± SEM*	fRPE ND ± SEM
59	5:03	32:48	Respiratory failure	None noted	None noted	12.84 ± 0.28^{3}	15.27 ± 0.31
67	6:49	45:36	Stroke	None noted	None noted	16.99 ± 0.40^{2}	3.66 ± 0.25
68	4:30	27:16	Lung cancer	No drusen noted; variable choroidal thinning	No drusen; more choroidal thinning than fellow explant with loss of choroidal vessels	$2.29 \pm 0.0.30^{2}$	28.90 ± 0.23
68	3:22	44:27	Sepsis	Unknown (poor RPE preservation)	Unknown (poor RPE preservation)	6.19 ± 0.38^{1}	19.54 ± 0.29
69	4:55	31:15	Renal failure	Small drusen	Small drusen	0.61 ± 0.08^{1}	1.19 ± 0.10
69	3:54	30:20	COPD	None noted	None noted	3.47 ± 0.30^{2}	16.81 ± 0.39
70	5:03	47:40	Sepsis	Few small drusen	Few small drusen; heavy BLinD	0^{3}	0
71	2:30	42:00	Intra-abdominal abscess	No drusen noted; heavy BLinD	No drusen noted; heavy BLinD	0^{1}	16.53 ± 0.25
71	4:40	28:10	Sepsis	Few small drusen	Few small drusen	0^{2}	29.68 ± 0.33
73	5:31	46:31	Acute respiratory distress syndrome	Few small drusen; heavy BLinD	Few small drusen	0^{2}	0
74	5:55	24:55	COPD	Heavy BLinD forming superficial lumps; choroidal thinning	Heavy BLinD forming superficial lumps; choroidal and cc degeneration in central macula	2.92 ± 0.43^{1}	18.27 ± 0.49
74	3:45	48:55	Respiratory failure	None noted	None noted	2.25 ± 0.35^{1}	15.12 ± 0.28
74	3:45	42:30	Metastatic lung cancer	None noted	None noted	8.55 ± 0.38^{2}	15.18 ± 0.40
75	4:38	33:48	Renal failure	Several small drusen	Several small drusen	0^{3}	8.02 ± 0.38
76	5:27	29:53	Septic shock	None noted	None noted	0^{2}	7.26 ± 0.30
76	6:00	42:55	Intracerebral hemorrhage	Few small drusen	Few small drusen (<fellow explant)	2.21 ± 0.25^{2}	12.47 ± 0.49
77	5:17	43:00	Hypertension	None noted	None noted	10.36 ± 0.35^{3}	12.70 ± 0.37
79	3:14	29:49	Pneumonia	None noted	None noted	0^{1}	2.97 ± 0.22
79	4:30	47:00	Pneumonia	None noted	None noted	0^{3}	18.32 ± 0.24
80	4:50	42:55	Cancer (type unknown)	None noted	No drusen noted; severe degeneration of the cc and choroidal vessels	5.58 ± 0.25^{1}	7.00 ± 0.50
81	5:30	42:30	Acute cardiac crisis	Large and small drusen	Unknown (poor RPE preservation)	0^{1}	0
87	6:10	36:45	Cardiac arrest	Few small drusen; heavy BLinD	No drusen noted; heavy BLinD	0^{3}	2.69 ± 0.41
93	4:05	46:55	Cardiac arrest	None noted	None noted	NA†	NA†

All donor eyes exhibited basal linear deposits (BLinD) extending into the inner collagenous layer of Bruch's membrane. Explants with substantial deposits are noted above. D to P, death to preservation; D to R, death to receipt; COD, cause of death; ND, nuclear density (nuclei/mm Bruch's membrane); SEM, standard error of the mean; COPD, chronic obstructive pulmonary disease; BLinD, basal linear deposits; cc, choriocapillaris.

* Superscript after ND indicates the batch of hES-RPE.

† Data available for equatorial explants only (submacular explants contaminated).

moval[31] and is the surface likely to be encountered in AMD donors with evolving atrophy if drusen are removed mechanically before cell transplantation.) Six-millimeter diameter punches from the submacular and equatorial nasal regions of fellow eyes were obtained using a trephine (Storz Instruments; Bausch and Lomb, Inc., Rochester, NY), creating an organ explant consisting of sclera and choroid. Equatorial explants were glued with tissue adhesive spots (Vetbond; 3M, St. Paul, MN) applied with a 10-μL pipettor along the perimeter of the explant to prevent choroid detachment from the sclera during culture. Glued explants were rinsed three times (10 minutes each) in phosphate buffered saline (PBS) containing 2.5 μg/mL amphotericin B and 50 μg/mL gentamicin or 50 μg/mL Normocin (InvivoGen, San Diego, CA). Preliminary studies comparing fRPE survival on glued versus not glued equatorial explants showed no difference in cell survival (data not shown). Submacular explants (gluing was not necessary because of the tight adherence of the choroid to the sclera) were rinsed once in PBS with the aforementioned supplements. Explants were placed in wells of 96-well tissue culture plates for cell seeding and organ culture.

Experimental Design

One submacular and zero to three equatorial BM explants were prepared from each donor eye to optimize tissue and cell use. Explants were seeded with approximately 3164 cells/mm^2 of fRPE harvested from tissue culture plates using trypsin or hES-RPE recovered from thaw. This seeding density produces a complete monolayer of cells 1 day after seeding.[12] The number of cells seeded with hES-RPE was calculated based on the number of live cells present after thaw (trypan blue exclusion test). The percent of live cells recovered from thaw was 81.6 ± 0.10% for hES-RPE1 (N = 7), 74.1 ± 0.12% for hES-RPE2 (N = 7), and 86.8 ± 0.10% (N = 6) for hES-RPE3. When three equatorial BM explants were prepared from the same donor eye, two different batches of hES-RPE were seeded on adjacent explants, and fRPE were seeded on the remaining equatorial explant. Equatorial explants were cultured for 1 day to assess initial attachment (N = 5, hES-RPE1; N = 6, hES-RPE2; N = 5, hES-RPE3; N = 10, fRPE) or 21 days to assess long-term survival (N = 10, hES-RPE1; N = 8, hES-RPE2; N = 5, hES-RPE3; N = 19, fRPE). The 21-day time point was chosen over 14 days as an endpoint for long-term survival because our previous studies showed that cells at day 14 appeared to be in transition, with many cells that appeared to be dying.[13,29] Because the nuclear density counts include cells that would be in a transition state, nuclear density counts at day 14 in organ culture could be misleading. Therefore, the 21-day time point is a more definitive end point to assess cell survival on BM in this organ culture paradigm.

Submacular explants were seeded with one hES-RPE batch, and the submacular explant from the fellow eye was seeded with fRPE (N = 8, hES-RPE1; N = 8, hES-RPE2; N = 6, hES-RPE3; N = 22, fRPE). Submacular explants were cultured for 21 days. Explants with hES-RPE were cultured in "stem cell" media (KO-DMEM, 1% nonessential amino acids, 2 mM GlutaMax, 0.1 mM mercaptoethanol, 7% serum replacement [all from Invitrogen, Life Technologies]), 5% fetal bovine serum, 100 μg/mL Normocin). hES-RPE grown in this medium have been well characterized and are similar to in situ RPE.[9] Explants seeded with fRPE were cultured in RPE media, media that has been used to characterize fRPE behavior on aged and AMD BM.[4,12,13] Media was changed for all explants three times per week. Explants were harvested at 1 or 21 days and placed in fixative (phosphate buffered 2% paraformaldehyde, 2.5% glutaraldehyde). Explants were bisected to process one half for light microscopy (LM) and the other half for scanning electron microscopy.

Light Microscopy of BM Explants

Explant halves to be processed for histology were embedded in resin (LR White; Electron Microscopy Supply, Chestnut Hill, MA); four to six sections of 2-μm thickness were mounted on slides and dried overnight. Sections were stained with 0.03% toluidine blue.[29] LM evaluation focused on RPE morphology (cell shape, density, and differentiation features), BM morphology, and evaluation of the explant integrity. Nuclear density counts were performed on four to five nonadjacent slides as described previously.[13] Nuclear densities rather than cell counts were assessed to compare cell attachment because of the difficulty in discerning cell boundaries between very flat cells. Linear measurements of BM in the analyzed areas were obtained by digital image acquisition and measurement with the freehand line tool of NIH ImageJ (developed by Wayne Rasband, National Institutes of Health, Bethesda, MD; available at http://rsb.info.nih.gov/ij/index.html). Differences in nuclear densities between paired data (hES-RPE versus fRPE) were tested for normal distribution (Shapiro–Wilk normality test) before comparison analyses by paired t-test or Wilcoxon signed rank test. Comparisons between hES-RPE preparations or fRPE batches within each time point were performed by one-way analysis of variance (ANOVA) and all pairwise multiple comparison procedures (Holm–Sidak method) if statistically significant differences were determined. Nonparametric testing of hES-RPE or fRPE nuclear densities within a time point was performed with the Kruskal–Wallis one-way ANOVA. Statistical differences between time points or equatorial versus submacular nuclear densities were determined by the unpaired t-test or Mann-Whitney rank sum test. $P < 0.05$ was considered statistically significant. Commercial software (SigmaPlot 11; Systat Software, Inc., San Jose, CA) was used for statistical analysis.

Scanning Electron Microscopy of BM Explants

Specimens for scanning electron microscopy (SEM) were dehydrated, critical point dried, and sputter-coated according to standard protocols. Samples were examined with a scanning electron microscope (JEOL JSM 35C, Tokyo, Japan, retrofitted with a digital image acquisition system [Gatan, Pleasanton, CA] or a JEOL JSM 6510), and were routinely photographed at 30× and 50× for low magnification evaluation. In addition, four fields were photographed at 200× and 1000× in the submacular region and in the center of equatorial explants. SEM evaluation compared surface morphology of cells, determined surface coverage, and confirmed the level of debridement of native RPE and RPE basement membrane in areas not resurfaced by cells.

Immunochemical Staining and Confocal Analysis

To further characterize cell behavior on aged submacular BM, immunochemical staining and confocal microscopy was performed using submacular BM explants seeded with hES-RPE2 or hES-RPE3 and fRPE. Explants were prepared from 17 donor eye pairs (mean age ± SEM, 79.0 ± 0.343 years) and harvested at day 3 (hES-RPE 2, N = 4; hES-RPE3, N = 2; fRPE, N = 6), day 7 (hES-RPE2, N = 1; hES-RPE3, N = 4; fRPE, N = 5), day 14 (hES-RPE2, N = 2; fRPE N = 6), and day 21 (fRPE, N = 4). All donor eyes had no to few submacular drusen except one AMD donor pair used for a day 3 study (hES-RPE3 versus fRPE). After culture in stem cell or RPE media, explants were washed three times with PBS and fixed overnight in buffered 4% paraformaldehyde at 4°C. After fixation, explants were cut into quarters to allow for multiple marker visualization and washed three times with PBS. Explant quarters were then incubated for 1 hour at room temperature in blocking solution (2% normal goat serum, 0.5% BSA, and 0.1% Triton X-100 in PBS). Primary antibodies diluted in blocking solution (1:200 dilution of rabbit polyclonal microphthalmia-associated transcription factor, MITF [Abcam, Cambridge, MA], 1:50 dilution of mouse monoclonal cellular retinaldehyde binding protein, CRALBP [Abcam], 1:100 dilution of mouse monoclonal pancytokeratin [Sigma Aldrich], 1:50 dilution of rabbit polyclonal Ki-67 [Abcam]) were applied to explant quarters for overnight incubation at 4°C. The following day, explants were washed three times in PBS. Secondary antibodies in blocking solution (1:32 dilution of fluorescein [FITC] goat anti-mouse IgG [Sigma Aldrich] or 1:50 dilution of FITC goat anti-mouse IgG and rhodamine [TRITC] goat anti-rabbit IgG [Jackson ImmunoResearch Laboratories, West Grove, PA]) were applied, and explant quarters were incubated for 1.5 hours at room temperature. After PBS washing, the nuclear stain, TO-PRO-3 (Molecular Probes, Eugene, OR), was

applied for 15 minutes followed by three 10-minute PBS washes. For TUNEL staining, explant quarters were permeabilized in 0.1% triton in 0.1% sodium citrate for 2 minutes on ice, washed with PBS, and incubated in TUNEL staining mixture (In Situ Cell Death Detection Kit, TMR red; Roche, Indianapolis, IN) for 1 hour at 37°C. After TUNEL staining, explant quarters were secondarily stained for cytokeratin and nuclei counterstained with TO-PRO-3. Negative controls for immunostaining were equatorial explants seeded with or without cells with no or secondary antibodies only and submacular explant quarters with no antibodies. Positive controls for TUNEL were equatorial explants seeded with cells, treated with 300 U/mL DNase I (Roche) according to the manufacturer's protocol before TUNEL staining. All controls with seeded cells were counterstained with TO-PRO-3. Explants were stored and examined in mounting medium (Vectashield; Vector Laboratories, Burlingame, CA). Explants were imaged using a 40× water immersion lens on a confocal microscope (LSM510; Zeiss, Thornwood, NY). Single 1-μm z-sections were acquired from cells on the surface of BM using the multitrack mode. Lasers lines and corresponding emission filters were: 488 nm excitation, 505 to 530 nm band pass filter for FITC; 543 nm excitation, 560 to 615 nm band pass filter for TRITC; 633 nm excitation, and 650 nm long pass filter for TO-PRO-3. After confocal analysis, explants were postfixed in mixed aldehyde fixative and processed for SEM as described previously.

Analysis of Integrin mRNA Expression

Cells harvested but not seeded on explants were frozen in reagent (RNAlater; Qiagen, Valencia, CA) for real time PCR analysis of RPE markers (bestrophin and MITF), and integrins αv, α1–6, β1, and β3–6. Total RNA was extracted from hES-RPE1 through hES-RPE3 and from four fRPE cultures using an RNA extraction kit (RNeasy, Qiagen). Following reverse transcription of RNA using a high capacity cDNA reverse transcription kit (Applied Biosystems, Foster City, CA), real-time PCR was performed (7500 Real-Time PCR System; Applied Biosystems) using assay kits (TaqMan Gene Expression Assay kit; Applied Biosystems) prepared for human integrin subunits, bestrophin, and MITF (proprietary primer and probe sequences). The relative level of gene expression was determined by the comparative cycle threshold (C_t) method with each sample normalized to 18s rRNA and expressed as a relative change. Each sample was run in triplicate. Results were averaged and expressed as relative amounts. Comparisons were made between samples processed at the same time.

Protein Secretion Analysis

Media overlying BM explants in organ culture was changed at day 19 (48 hours before collection at day 21). Collected media (approximately 200 μL) were centrifuged briefly to remove cells and cellular debris, and supernatant was stored frozen at −80°C. Media was analyzed for secreted proteins using a custom multiplex testing service (Searchlight; Pierce Biotechnology, Woburn MA). Based on preliminary data examining protein secretion in RPE-conditioned media from two day 21 fRPE cultures on BCE-ECM (data not shown), media was tested for VEGF-A, pigment epithelium derived factor (PEDF), transforming growth factor (TGF)-β2, insulin growth factor binding protein (IGFBP)-3, and thrombospondin (TSP)-2, all of which were shown to be in relatively high concentration (nanogram and microgram [PEDF only] quantities/mL conditioned media). In addition, we tested for the presence of the following, identified in picogram per mL amounts in RPE-conditioned media: nerve growth factor (NGF), brain-derived neurotrophic factor (BDNF), platelet-derived growth factor (PDGF)-β, and TNF-α. Control samples included stem cell or RPE media with no previous exposure to explants or cells ($N = 4$ for each media) and stem cell or RPE media overlying equatorial explants with no hES-RPE or fRPE seeding ($N = 4$ for each media, donor age 74.0 ± 9.02 years). Equatorial BM explant controls were from the same donors whose submacular and equatorial BM was seeded with fRPE and hES-RPE. Submacular explants ($N = 5$, donor age 82.8 ± 8.96 years) were from donor eyes prepared specifically to determine the choroid/sclera secretion of submacular explants and included two donor pairs with no submacular pathology and three donor pairs with varying amounts of drusen. To determine whether there was a statistical difference in the amount of protein measured in conditioned media harvested at day 21 from the different cell preparations, protein levels were compared by Kruskal–Wallis one-way ANOVA on ranks with multiple comparison testing by all pairwise multiple comparison procedures (Dunn's method). $P < 0.05$ was considered statistically significant.

Results

Day 1 Equatorial BM Explants

At day 1, nuclear densities of fRPE on equatorial explants ranged from 6.79 to 20.49 nuclei per millimeter of BM (mean nuclear density ± SEM, 14.39 ± 4.55; Fig. 1). For hES-RPE, nuclear densities for hES-RPE1 ranged from 5.37 to 15.65 nuclei per millimeter of BM (mean nuclear density ± SEM, 12.18 ± 1.97); for hES-RPE2, nuclear densities ranged from 2.92 to 10.92 nuclei per millimeter of BM (mean nuclear density ± SEM, 6.21 ± 1.24); and for hES-RPE3, nuclear densities ranged from 3.89 to 8.49 nuclei per millimeter of BM (mean nuclear density ± SEM, 6.18 ± 0.84). Nuclear densities of all batches of hES-RPE were significantly different from fRPE seeded onto fellow eye BM explants (paired t-test; $P < 0.05$; see Fig. 1). One-way ANOVA revealed no nuclear density differences among fRPE seeded onto different explants. There were significant differences in nuclear density among batches of hES-RPE ($P = 0.016$). All pairwise multiple comparison procedures testing (Holm–Sidak method) showed that hES-RPE1 nuclear densities were significantly higher than hES-RPE2 ($P = 0.010$) and hES-RPE3 ($P = 0.012$); hES-RPE2 and hES-RPE3 nuclear densities were not significantly different from each other ($P = 0.987$). There were no significant differences in donor ages for explants seeded with the different batches of hES-RPE (one-way ANOVA; $P = 0.950$).

At day 1, 9 of 11 explants seeded with fRPE showed complete (Figs. 2A, B) or almost complete resurfacing (Figs. 3A, B) by confluent cells with small defects in cell coverage. Confluent areas exhibited large, flat cells with smooth surfaces or short apical processes. Some explants showed RPE multilayer-

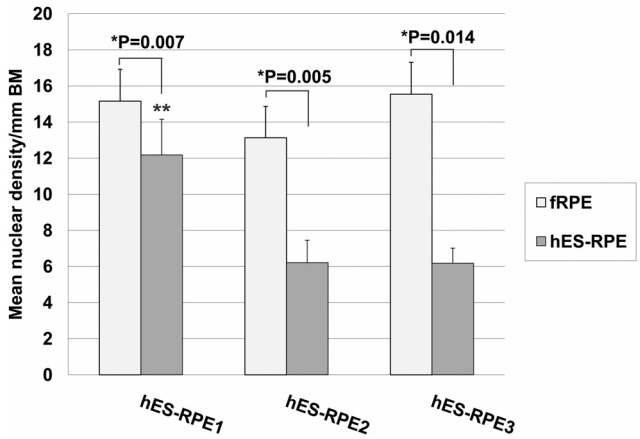

Figure 1. Nuclear density (mean nuclei/mm Bruch's membrane ± SEM) of paired explants seeded with fetal RPE (fRPE) or human embryonic stem cell–derived RPE (hES-RPE) of different degrees of pigmentation, 1 day after seeding on aged equatorial Bruch's membrane (hES-RPE1, $N = 5$; hES-RPE2, $N = 6$; hES-RPE3, $N = 5$; fRPE, $N = 10$). Nuclear density was significantly lower (*) for explants seeded with hES-RPE compared to the nuclear density of fRPE seeded on fellow eye explants. Nuclear density of hES-RPE1 (**) was significantly higher than that of hES-RPE2 ($P = 0.010$) and hES-RPE3 ($P = 0.012$).

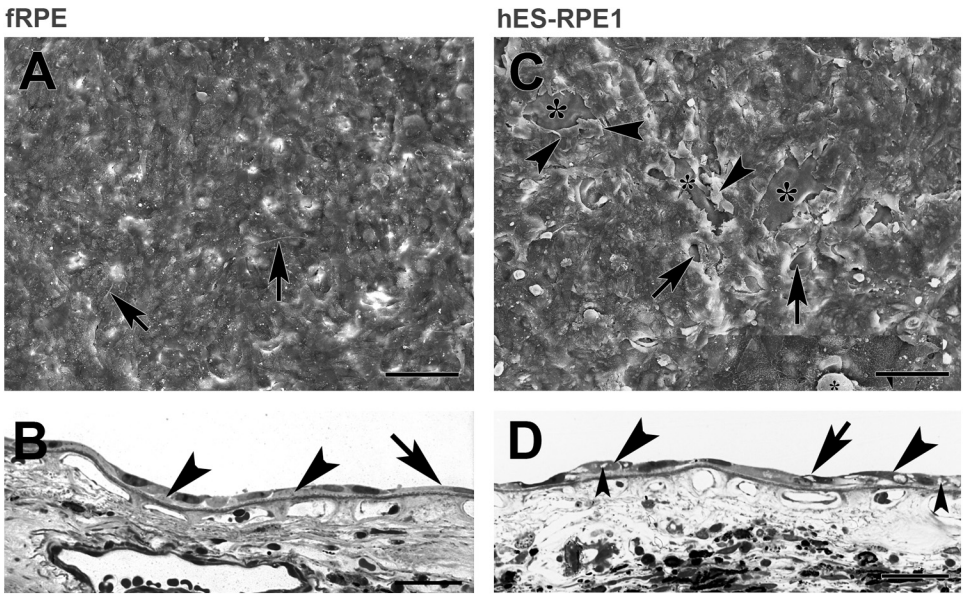

FIGURE 2. fRPE and hES-RPE1 resurfacing of equatorial Bruch's membrane explants from a 69-year-old donor after 1 day in culture. (**A**) Scanning electron micrograph (SEM) shows that flat, confluent fRPE fully resurface the explant with small intercellular gaps (nuclear density [ND], 18.52 ± 0.54). Short apical processes are present on the flattened surfaces of the cells. Some of the cells exhibit lamellipodia (*arrows*). (**B**) Light micrograph (LM) of explant seeded with fRPE showing cell variability in size and shape. The cells adhere closely to the inner collagenous layer (ICL). Cells overlie adjacent cells (*left arrowhead*) or extend processes over adjacent cells (*right arrowhead*). A very elongate cell is indicated by the *arrow*. (**C**) SEM of explant seeded with hES-RPE1 shows almost complete resurfacing of the explant with a few small defects (*arrows* point to some of the defects). In some areas, the cells appeared to have fallen off (*asterisks*). The cells are highly variable in size and shape. The poor attachment of cells is indicated by areas where the cells appear to be peeling off the explant (*arrowheads*; ND, 15.54 ± 0.33). (**D**) LM of an explant seeded with hES-RPE1 shows cells lying on top of other cells on Bruch's membrane (*large arrowheads*). Several of the cells have vacuoles (*small arrowheads*). The *arrow* points to a lamellipodia extending over an adjacent cell. Scale bar: (**A**, **C**) 100 μm; (**B**, **D**) 30 μm. Toluidine blue staining.

ing in localized areas. Cells were highly variable in size and shape. Large elongate cells were sometimes present on top of monolayers or adjacent to areas where defects were located. Short filopodia and lamellipodia were not uncommon, extending over adjacent cells. The two remaining explants showed poor resurfacing with single rounded or flattened cells or patches of confluent cells.

Regardless of the degree of pigmentation, hES-RPE resurfacing of BM was by cells of highly variable size and morphology (e.g., single cells that were round [sometimes ballooned, fragmented, or with cell membrane holes], elongate, or slightly flattened with multiple lamellipodia); incomplete resurfacing by patches of large, smooth, flattened cells often with lamellipodia extending over adjacent cells was also observed (Fig. 2D). Lamellipodia were often much longer than those observed in fRPE at the same time point. On some explants, the cells did not appear to be very well attached (Fig. 2C). Of the three hES-RPE preparations, hES-RPE1 appeared to be the most successful at resurfacing equatorial BM at day 1 after seeding (Figs. 2C, D). Specimens with hES-RPE2 and hES-RPE3 displayed

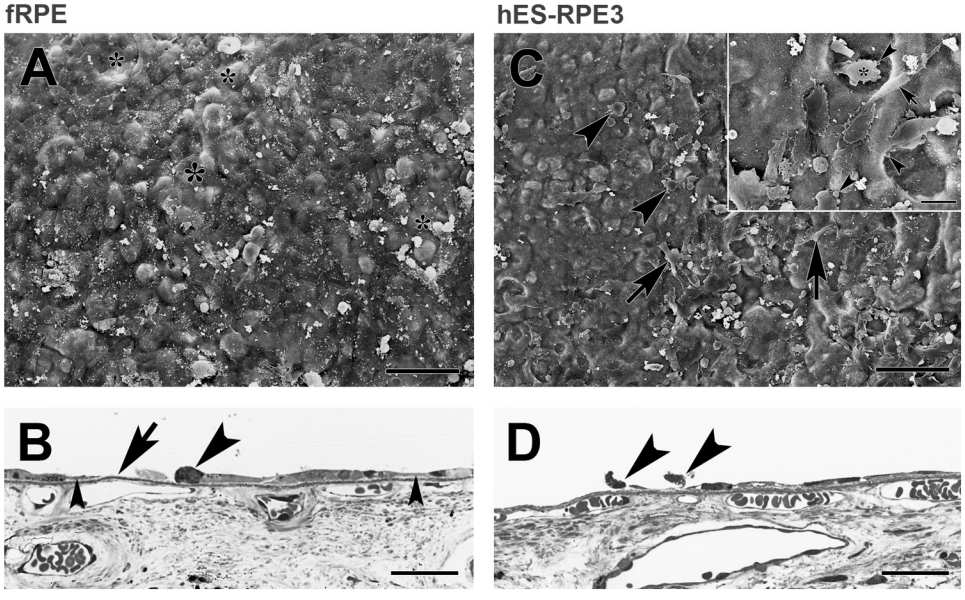

FIGURE 3. FRPE and hES-RPE3 resurfacing of equatorial Bruch's membrane explants from a 76-year-old donor after 1 day in culture. (**A**) SEM of an explant seeded with fRPE (ND, 15.38 ± 0.31). FRPE incompletely resurfaced the explant with large, very flat cells. Some of the larger areas not resurfaced are indicated by an *asterisk*. Because the cells are so flat, cell edges along defects are difficult to see at this magnification. (**B**) LM of the explant shows the variable morphology of fRPE on Bruch's membrane that is incompletely resurfaced. A rounded, condensed cell (*arrowhead*) is adjacent to a defect in coverage (*large arrow*). A single cell lies between the *arrow* and *large arrowhead*. *Small arrowheads* point to thin cell processes extending along Bruch's membrane. (**C**) SEM of explant seeded with hES-RPE3 (ND, 4.70 ± 0.55). The explant is poorly resurfaced primarily by single cells that are rounded and not well attached, elongate cells (*arrows*), and cells that are partially spread with blebs (*arrowheads*). *Inset*: higher magnification shows most of the explant is unresurfaced ICL. Cell blebbing (*arrowheads*) is noticeable at this magnification with some cells exhibiting many blebs (*asterisk*). *Arrow* points to a very elongate cell. (**D**) LM of the explant in an area with cells (most of the explant has no cells) shows the limited attachment by hES-RPE3. *Arrowheads* point to cells that appear to be falling off the explant. Scale bar: (**A**, **C**) 100 μm; (**C**, inset) 20 μm; (**B**, **D**) 30 μm. Toluidine blue staining.

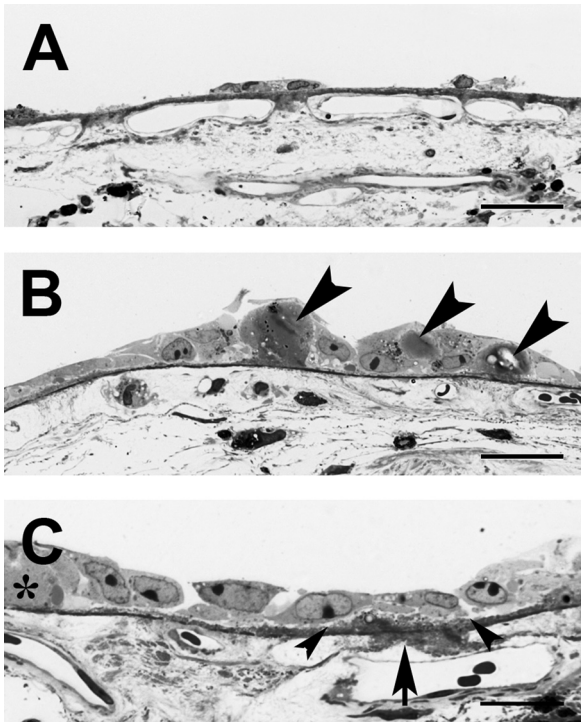

FIGURE 4. fRPE and hES-RPE1 resurfacing of an AMD equatorial Bruch's membrane from a 77-year-old donor 1 day after seeding. (**A**) hES-RPE1 attached to the ICL of this donor explant to a limited degree. The few cells that are present on the explant are not well spread. Bruch's membrane shows basal linear deposit extending into the intercapillary pillars (ND, 5.37 ± 0.45). (**B**) fRPE seeded onto an adjacent explant effectively resurfaced the explant with enlarged cells (compare with fRPE in Figs. 2B and 3B). Cells attached and spread over drusen (*arrowheads*; ND, 9.50 ± 0.31). (**C**) Enlarged fRPE attached to heavy basal linear deposit forming lumps on the surface of the ICL (area of heavy deposits is located between arrowheads). In this field, the basal linear deposit extends from the ICL well into the intercapillary pillars (*arrow*) with deposit extending under the outer surface of the choriocapillaris endothelium and its basement membrane, filling the gap between the choriocapillaris and a deeper choroidal vessel. A small druse (*asterisk*) is resurfaced by cells. Scale bar: (**A**, **B**) 30 μm; (**C**) 20 μm. Toluidine blue staining.

abundant single cells that were either poorly attached or showed limited spreading on the ICL (Figs. 3C, D). Cell membrane blebs often were present on these single cells (Fig. 3C, inset).

All explants showed some degree of aging changes in BM, ranging from a thickened elastic layer to basal linear deposit spread from the ICL into the intercapillary pillars. The degree of attachment and spreading by fRPE did not appear to be related to the amount of basal linear deposit in BM, but seemed to affect hES-RPE attachment and spreading in some cases. For example, in two explants from the same donor, seeded with hES-RPE1 (Fig. 4A) or fRPE (Figs. 4B, 4C), basal linear deposit accumulation was substantial, forming lumps on the surface of the ICL. fRPE almost completely resurfaced this explant, while the fellow explant showed the poorest resurfacing of the explants seeded with hES-RPE1. Of explants seeded with fRPE, only one explant had numerous large drusen. fRPE attached and spread on the drusen, but in general, cells in these areas were abnormal (large and ballooned; Figs. 4B, 4C). Because of the poor attachment and spreading of hES-RPE2 and hES-RPE3, the effect of drusen on resurfacing of explants by hES-RPE was difficult to determine.

Day 21 Equatorial BM

At day 21, nuclear densities of fRPE on equatorial explants ranged from 0 to 29.44 nuclei per millimeter of BM (mean nuclear density ± SEM, 13.22 ± 2.36; Fig. 5). For hES-RPE1, nuclear densities ranged from 0 to 6.14 nuclei per millimeter of BM (mean nuclear density ± SEM, 1.34 ± 0.80). Of the 10 explants seeded with hES-RPE1, seven had no remaining cells. Despite poor resurfacing at day 1 compared to hES-RPE1 (Fig. 1), hES-RPE2 and hES-RPE3 were able to resurface equatorial explants to a greater degree at day 21. hES-RPE2 nuclear densities ranged from 0.56 to 34.12 nuclei per millimeter of BM (mean nuclear density ± SEM, 12.03 ± 3.82); hES-RPE3 nuclear densities ranged from 2.52 to 15.44 nuclei per millimeter of BM (mean nuclear density ± SEM, 11.27 ± 2.75). hES-RPE2 and hES-RPE3 resurfaced equatorial BM explants to a similar degree as fRPE ($P = 0.059$ and 0.377, respectively; paired *t*-test). Nuclear density was significantly lower on paired explants seeded with hES-RPE1 compared to fellow explants seeded with fRPE ($P = 0.016$l; paired *t*-test). One-way ANOVA showed a statistically significant difference in the nuclear density among the hES-RPE batches ($P = 0.003$). All pairwise multiple comparison procedures (Holm–Sidak method) showed hES-RPE1 nuclear density to be significantly lower than that of hES-RPE2 and hES-RPE3; hES-RPE2 and hES-RPE3 nuclear densities were not statistically different from each other (Fig. 5). Nuclear density of hES-RPE1 on equatorial explants at day 21 was significantly lower than the nuclear density on equatorial explants at day 1 ($P = 0.004$, Mann-Whitney rank sum test). Nuclear densities on equatorial explants were not statistically different at day 1 and day 21 for fRPE ($P = 0.654$; Mann-Whitney rank sum test), hES-RPE2 ($P = 0.236$; unpaired *t*-test), or hES-RPE3 ($P = 0.690$; Mann-Whitney rank sum test). There were no significant differences in donor ages for explants seeded with the different batches of hES-RPE (Kruskal–Wallis one-way ANOVA; $P = 0.570$).

As previously noted, BM explants were highly variable in the amount of basal linear deposit present. Generally, BM explants showed some accumulation of basal linear deposit, ranging from mild deposition causing thickening of the elastic layer to substantial deposition extending into and sometimes through the intercapillary pillars. The amount and extent of

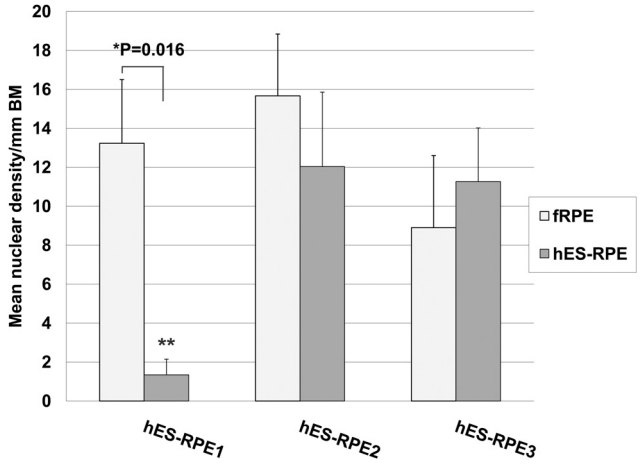

FIGURE 5. Nuclear density of fRPE versus hES-RPE of different degrees of pigmentation on aged equatorial Bruch's membrane at day 21 in organ culture (hES-RPE1, $N = 10$; hES-RPE2, $N = 8$; hES-RPE3, $N = 5$; fRPE, $N = 18$). fRPE nuclear density was significantly higher than that of hES-RPE1 ($^*P < 0.05$) but not hES-RPE2 or hES-RPE3. hES-RPE1 nuclear density was significantly lower than that of hES-RPE2 and hES-RPE3 ($^{**}P < 0.05$).

basal linear deposit did not appear to affect either hES-RPE or fRPE survival, with the exception of 1 explant. This explant, seeded with hES-RPE2, showed the highest nuclear density of all 21-day equatorial explants (34.12 nuclei/mm of BM). The explant was characterized by a severely degenerate choriocapillaris and choroid with no discernable sublaminae in BM and no basal linear deposit. Although the presence of equatorial drusen did not appear to impair overall fRPE survival compared to RPE survival on explants without equatorial drusen, localized resurfacing over equatorial drusen was poor, ranging from bare drusen with no overlying cells, to drusen overlaid with abnormal cells, to drusen covered by very thin cell extensions.

Of the explants seeded with hES-RPE1 with cells remaining at day 21, the explants were sparsely resurfaced with enlarged, elongate cells, some with short apical processes. Nuclei were generally flattened (Figs. 6A, B). hES-RPE2 and hES-RPE3 cells variably resurfaced all equatorial explants at day 21 in organ culture. In explants with few remaining cells, these cells tended to be isolated, rounded, ballooned cells. Explants with a higher degree of resurfacing showed large, polymorphic, flat and/or elongate cells (Figs. 6C, 6D). Cell surfaces were either smooth or with short apical processes. Nuclei were variable in morphology: flattened and condensed, round and enlarged, or irregularly shaped. Cells with loss of cytoplasm or vacuoles were not uncommon in all preparations of hES-RPE (Fig. 6).

In BM explants with the most resurfacing by fRPE, morphology was still highly variable but not as irregular or abnormal as hES-RPE morphology (Fig. 7). Morphology ranged from large, flattened, or spindle-shaped to compact, flat cells in explants with the most resurfacing. Short apical processes on the surface of the cells or along cell borders could be seen on some, but not all cells. fRPE were generally healthier without loss of cytoplasm commonly seen in hES-RPE resurfaced explants. In areas of highest density, cells were confluent, but cell size and nuclear shape were variable with some localized areas of multilayering.

The innermost regions of equatorial explants were well preserved at day 21 with intact BM sublaminae (see light micrographs at this time point [Figs. 6B, 6D, 7B]). In general, choroidal preservation at day 21 was similar to that observed in equatorial explants at day 1; choroidal fiber disruption was not uncommon in the region adjacent to the sclera with varying degrees of detachment of the choroid from the sclera. Intact choroidal cells were present at both time points. However, compared to day 1 equatorial explants, choriocapillaris endothelial cells were not as well preserved.

Day 21 Submacular BM

At day 21, nuclear densities of fRPE on submacular explants ranged from 0 to 29.69 nuclei per millimeter of BM (mean nuclear density ± SEM, 11.43 ± 1.89; Fig. 8). For hES-RPE1, nuclear densities ranged from 0 to 6.19 nuclei per millimeter of BM (mean nuclear density ± SEM, 2.19 ± 0.90). hES-RPE2 nuclear densities ranged from 0 to 16.99 nuclei per millimeter of BM (mean nuclear density ± SEM, 4.19 ± 2.08). hES-RPE3 nuclear densities ranged from 0 to 12.84 nuclei per millimeter of BM (mean nuclear density ± SEM, 3.87 ± 2.47). fRPE nuclear density on aged submacular BM was significantly higher than fellow submacular explants seeded with hES-RPE1 (Fig. 8; $P = 0.016$; Wilcoxon signed rank test). Paired *t*-tests showed no significant differences between fRPE and hES-RPE2 seeded on fellow eye explants ($P = 0.079$) and no differences between fRPE and hES-RPE3 ($P = 0.096$). Nuclear densities of hES-RPE1, hES-RPE2, and hES-RPE3 were not significantly different from each other ($P = 0.840$; Kruskal-Wallis one-way ANOVA on ranks). Nuclear densities of fRPE paired with each batch of hES-RPE were also not significantly different from each other ($P = 0.551$; one-way ANOVA). Location of the explant (equatorial or submacular) was not associated with probability of survival of fRPE or any of the preparations of hES-RPE (equatorial versus submacular fRPE, $P = 0.813$ [Mann-Whitney rank sum test]; equatorial versus submacular hES-RPE1, $P = 0.131$ [Mann-Whitney rank sum test]; equatorial versus submacular hES-RPE2, $P = 0.182$ [unpaired *t*-test]; equatorial versus submacular hES-RPE3, $P = 0.076$ [unpaired *t*-test]). There were no significant differences in donor ages for explants seeded with the different batches of hES-RPE (one-way ANOVA; $P = 0.693$).

Submacular BM explant histology showed basal linear deposit in the inner and outer collagenous layers with basal linear

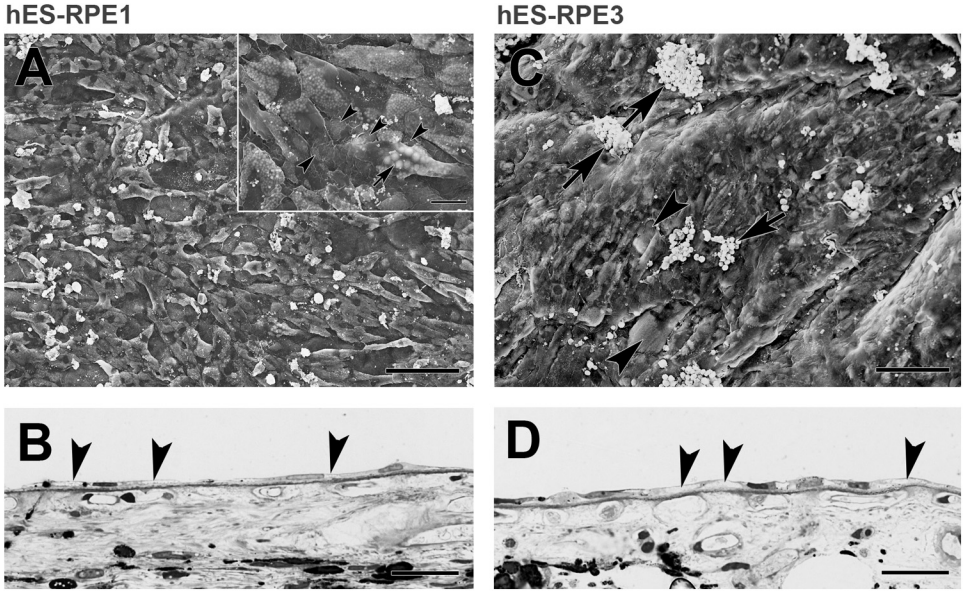

Figure 6. Morphology of hES-RPE on equatorial Bruch's membrane from a 59-year-old donor after 21 days in organ culture. (**A**) hES-RPE1 (ND, 6.10 ± 0.30). Cells incompletely resurface the explant with a mixture of large, elongate cells and enlarged, polymorphic cells. *Inset*: cells resurfacing the explant have smooth surfaces with no or few apical processes. At this magnification, small and large (*arrow*) vacuoles can be seen within many of the cells. The ICL is evident in regions with small defects in cell coverage (*arrowheads* point to some of the defects). (**B**) LM of the explant shows flattened, elongate cells on Bruch's membrane. *Arrowheads* point to part of flattened cells with vacuoles or loss of cytoplasm. (**C**) hES-RPE3 (ND, 15.44 ± 0.58). Cells almost completely resurfaced this explant with a few small defects in coverage (*arrowheads*). Cells are highly variable in size with varying degrees of vacuole formation. Rounded supernumerary cells are present on the surface of the monolayer (*arrows*). (**D**) LM shows hES-RPE3 resurfaced the explant with a monolayer of cells. Similar to the cells in **B**, vacuole formation and loss of cytoplasm are found in several of the cells (*arrowheads*). Scale bar: (**A**, **C**) 100 μm; (**A**, *inset*) 20 μm; (**B**, **D**) 30 μm. Toluidine blue staining.

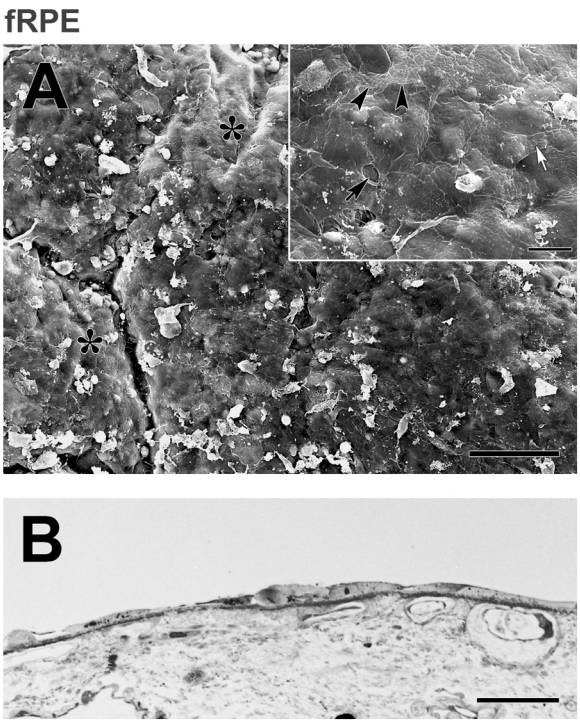

FIGURE 7. Morphology of fRPE on equatorial Bruch's membrane from a 59-year-old donor after 21 days in organ culture (same donor as Fig. 6). (**A**) fRPE incompletely resurfaced the explant with confluent patches of large, flat cells. Areas not fully resurfaced expose the inner collagenous layer (*asterisks*). Cell remnants are present (*white* debris; ND, 10.26 ± 0.41). *Inset*: The flattened appearance and smooth surfaces of the fRPE are more evident at this magnification. Unlike hES-RPE (Fig. 6), few vacuoles are present. A small intercellular gap is present (*arrow*). Cell extensions are not uncommon (*white arrow* points to lamellipodia extending over an adjacent cell). *Arrowheads* point to the border of a cell with a perforated cell membrane. (**B**) LM of the explant illustrates the variability in size and shape of fRPE. Scale bar: (**A**) 100 μm; (**A**, *inset*) 20 μm; (**B**) 30 μm. Toluidine blue staining.

deposit extending into the intercapillary pillars to varying degrees. Explants designated as "heavy basal linear deposit" in Table 1 showed multiple areas of basal linear deposit extending through the intercapillary pillars into the choroid and past the pillars to surround the outer surfaces of some choriocapillaris vessels. The presence of submacular drusen appeared to severely affect hES-RPE survival, regardless of the cell preparation. In general, all preparations of hES-RPE were capable of only limited resurfacing of submacular BM regardless of the extent of submacular pathology. fRPE showed limited resurfacing of three of four explants that exhibited substantial basal linear deposit accumulation and showed variable resurfacing of four of six explants with small (hard) drusen (see Table 1). hES-RPE with low nuclear densities on submacular BM were generally present as small patches of cells or single cells, often not well spread and often appearing damaged with membrane holes, apoptotic blebs, or loss of cytoplasm (Figs. 9A, B). Explants showing the most resurfacing by hES-RPE (3 explants seeded with hES-RPE2 or hES-RPE3) exhibited incomplete resurfacing by patches of cells with highly variable morphology (e.g., elongated, polymorphic, large, flat cells, and/or ballooned cells; Figs. 9C, 9D). Cells with vacuoles and/or loss of cytoplasm were not uncommon. Explants showing limited resurfacing by fRPE were partially resurfaced by cells often appearing better spread and attached to BM than explants with hES-RPE. With increasing resurfacing, fRPE formed confluent patches. However, morphology in general was highly variable, even within the same explant, ranging from small compact cells exhibiting short apical processes to enlarged cells to extremely large flat cells (Fig. 10). Vacuoles were seen in some fRPE, but were not as plentiful as in hES-RPE.

In general, preservation of submacular explants was better than that observed in equatorial explants at day 21. Submacular explants showed better preservation of choriocapillaris endothelial cells; the majority of explants retained choroidal attachment to the sclera, and preservation of choroidal fiber integrity was better.

Immunochemical and Morphologic Analysis at Days 3, 7, 14, and 21

Confocal analysis was performed on additional explants to determine whether cells on submacular BM maintain differentiation as RPE and whether cell death and/or proliferation contributed to the nuclear densities observed at day 21. Analysis of hES-RPE2 and hES-RPE3 on submacular explants was performed at days 3, 7, and 14 after seeding and compared to fRPE at the same time points seeded onto fellow eye explants. FRPE were also studied at day 21. hES-RPE1 was not studied because of the low survival on submacular explants at day 21 (see Fig. 8). Excess hES-RPE remaining after seeding onto explants and cultured in the same media as used on explants for 21 days, grew and resurfaced gelatin-coated tissue culture plates, assuring that inability to survive on BM was not related to poor cell viability. Viability of fRPE was also confirmed by growth of cells seeded onto BCE-ECM resurfaced tissue culture dishes and cultured in RPE media for the same period (data not shown.)

General Morphology. Confocal analysis followed by SEM evaluation revealed limited BM resurfacing by hES-RPE2 and hES-RPE3 at all time points studied while fRPE resurfacing, although initially high, declined with time in organ culture. Both hES-RPE preparations behaved similarly with limited spreading after attachment on BM. Mainly rounded and/or variably spread cells were attached on submacular BM at all time points with few small patches of cells in the best resurfaced explants at days 3 and 7 (Fig. 11). The day 3 AMD donor showed similar resurfacing to the other explants examined at this time point. The number of condensed and misshapen

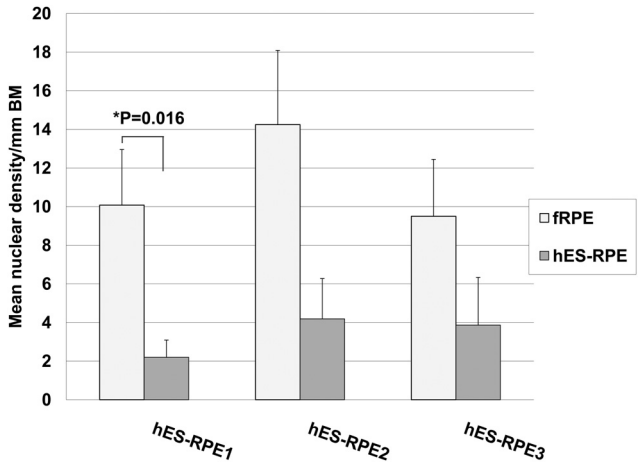

FIGURE 8. Nuclear density of paired submacular Bruch's membrane explants seeded with fRPE or hES-RPE of different degrees of pigmentation (hES-RPE1, $N = 8$; hES-RPE2, $N = 8$; hES-RPE3, $N = 6$; fRPE, $N = 22$) on submacular Bruch's membrane at day 21 after seeding. fRPE survival was significantly greater than hES-RPE1 seeded on fellow eye explants ($^*P < 0.05$). FRPE nuclear densities were not significantly different from those of hES-RPE2 and hES-RPE3 seeded on fellow eye explants ($P > 0.05$).

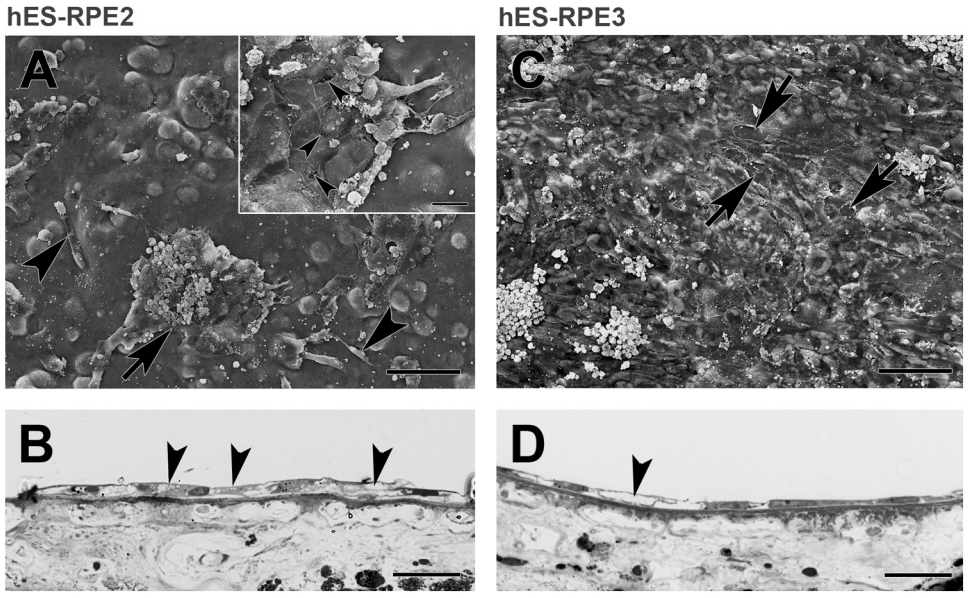

FIGURE 9. Morphology of hES-RPE2 and hES-RPE3 on submacular Bruch's membrane after 21 days in culture (**A**, **B** donor age 69 years; **C**, **D** donor age 59 years). (**A**) hES-RPE2 show limited resurfacing of the explant by cell patches and elongated single cells (*arrowheads*). Rounded dead cells can be seen on top of the patch indicated by an *arrow* (ND, 3.47 ± 0.30). High magnification inset shows cells within the patch have membrane holes (*arrowheads*). Cells along the edge of the patch appear to be dead or dying. (**B**) LM of cells within a patch. Many of the cells contain vacuoles or show loss of cytoplasm (*arrowheads*). (**C**) hES-RPE3 have almost completely resurfaced the explant with cells that are highly variable in size and shape. Small defects in the coverage are indicated by *arrows*. Clusters of dead cells are present on top of the cell monolayer (ND, 12.84 ± 0.28). (**D**) LM of the explant shows resurfacing by elongated, flat cells, some with loss of cytoplasm (*arrowhead*). Scale bar: (**A**, **C**) 100 μm; (**A**, *inset*) 20 μm; (**B**, **D**) 30 μm. Toluidine blue staining.

nuclei (evidenced by TO-PRO-3 staining) increased with time in culture. In some cases, the distribution of cells on explants from the same donor eye was not uniform, so some explant quarters had intact cells while others did not. At day 7, one explant had no remaining cells on submacular BM and cellular debris was present on the surface of two other explants. Small and large vacuoles were present in hES-RPE showing some degree of spreading (not rounded) at days 3 and 7. Generally, cells were more abundant on extramacular areas of the explants at both time points. At day 14, very few rounded hES-RPE were present on the two explants studied, so further study at this time point and later time points was not pursued.

fRPE were able to attach, spread, and form a fairly uniform surface covering of flat cells with small defects in coverage at day 3. The number and/or size of defects in the surface coverage increased with time in culture. fRPE exhibited abundant small vacuoles at day 3 with decreasing presence of vacuoles with increasing time in culture. At day 7, explants were resurfaced by healthy appearing cells of variable sizes, some with apical processes. At day 14, cell debris and cells with membrane holes were common. At day 21, impaired viability of cells was evident by cellular debris on the surface and nuclei of variable size and shape with some large (ballooned) and others shriveled and misshapen. One explant had a large defect involving most of the macula (see Fig. 12).

Immunochemical Analysis. CRALBP labeling of hES-RPE was seen in three explants at day 3 (summarized in Table 2). In addition to cytoplasmic label, some label was observed in nuclei. Labeling could not be determined on three explants because the cells on these quarter pieces appeared to be shriveled, and some cells did not appear to be intact. At day 7, CRALBP label was observed in the four explants with cells remaining on submacular BM. Labeling varied from few labeled cells to abundant labeled cells. The explant showing the most CRALBP-labeled cells was the explant with the most resurfacing (small patches of cells; see Fig. 11, day 7). Punctate nuclear MITF labeling with an occasional cell showing cytoplasmic label was found in two of five explants examined with cells remaining on the quarter explant pieces at day 3. At day 7, among the four explants with cells, all cells showed nuclear MITF labeling. Zero to few Ki-67–positive cells were seen at the two time points. Many cells were TUNEL-positive at day 3. TUNEL-positive cells were also observed at day 7. The majority of cells exhibited some cytokeratin staining at both time points, with some cells showing intense staining.

All fRPE were labeled for the RPE markers, CRALBP, and MITF at day 3. CRALBP labeled the cytoplasm with an occasional cell showing additional nuclear label. The majority of cells remained CRALBP-positive with time in culture while MITF was present in the nuclei of all cells at day 3 and decreased with time in culture. There did not appear to be a correlation between MITF-negative and CRALBP-negative cells (i.e., cells that were negative for MITF were not necessarily negative for CRALBP [see Fig. 12, day 14]). At all time points, occasional cells showed faint cytoplasmic in addition to nuclear MITF staining. At days 7 and 14, MITF labeling along cell borders was sometimes present. The presence of TUNEL-positive cells was highly variable between explants cultured for the same time period at days 3, 7, and 14, with some explants showing no label or few labeled cells while other explants showed localized areas of TUNEL-positive cells. At day 21, all explants showed some, but not many, TUNEL-positive cells. All day 3 explants showed abundant numbers of proliferating (i.e., Ki-67–labeled) cells, but the number of proliferating cells appeared to decrease with additional time in culture. Most, if not all, fRPE labeled positive for cytokeratin at day 3, with the

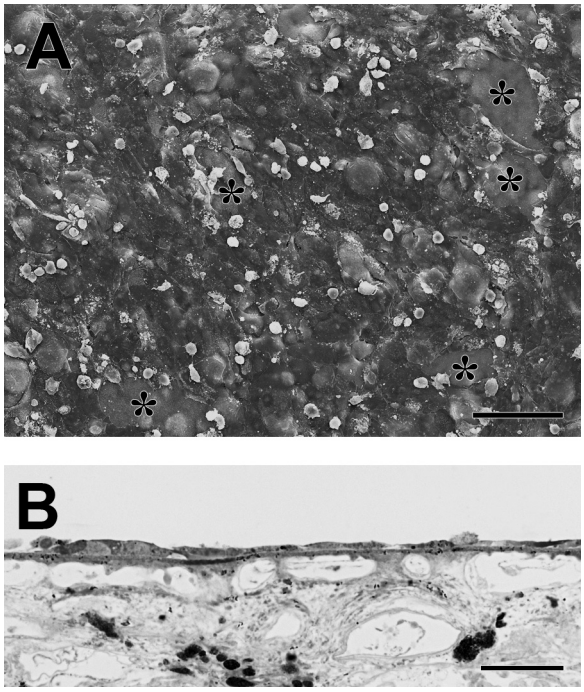

FIGURE 10. Morphology of fRPE on submacular Bruch's membrane after 21 days in organ culture (donor age 69 years, same donor as Fig. 9A, 9B). (**A**) fRPE show more resurfacing of the explant than that observed by hES-RPE on the fellow explant. Cells on the incompletely resurfaced explant are very flat and highly variable in size. Large defects in cell coverage are indicated by *asterisks* (ND, 16.81 ± 0.39). (**B**) LM of the explant shows the variability in cellular morphology. Scale bar: (**A**) 100 μm; (**B**) 30 μm. Toluidine blue staining.

majority of cells showing cytokeratin label at later time points. Intense cytokeratin staining was seen in some cells at all three time points.

FIGURE 11. hES-RPE behavior after 3- and 7-day culture on submacular human Bruch's membrane. Explants were immunostained for cytokeratin (FITC), MITF (rhodamine), CRALBP (FITC), Ki-67 (rhodamine), or TUNEL (rhodamine) followed by nuclear staining with the dye, TO-PRO-3 (blue). *Day 3*: hES-RPE3 on Bruch's membrane from a 74 year-old female with AMD. *SEM*: Single cells are present on the surface and are not well spread. *Cytokeratin*: Most cells stain positive for cytokeratin with some cells showing intense staining. Some of the cells contain condensed and misshapen nuclei. *MITF*: The majority of the cells show nuclear MITF staining with some cells showing faint cytoplasmic staining. *Arrow*: MITF-negative nucleus. *CRALBP*: Most, but not all cells, show CRALBP labeling of the cytoplasm. *Arrow*: CRALBP-negative cell. *Ki-67*, Ki-67–positive cells were seen rarely on this explant. *Arrow*: Ki-67–positive cell. *TUNEL + cytokeratin*: TUNEL-positive cells were abundant. In this field, all cells are TUNEL positive. *Day 7*: hES-RPE3 on Bruch's membrane from an 80-year-old female with few hard submacular drusen. *SEM*: Cells were present on this explant as single cells and as small patches of variably flattened cells. Vacuoles within flattened cells were common. *Cytokeratin*: The majority of cells showed some degree of cytokeratin staining although in some cells the staining was sparse. *MITF* (same field as cytokeratin): All cells on this explant were MITF-positive with occasional cells showing intense cytoplasmic labeling (*arrow*). *CRALBP*: Cells were not labeled as uniformly with CRALBP as at the earlier time point, and in some cells, the labeling was sparse. Abundant cellular debris is present on the surface of Bruch's membrane. *Ki67*: Ki-67–positive cells were in a few localized areas only. In this field, four cells are positively labeled (*arrows*). *TUNEL + cytokeratin*: Few TUNEL-positive nuclei were seen in cells present on the explant. *Arrow* points to one positive cell in a small cell patch. Scale bars: 20 μm.

Integrin mRNA Expression

To determine whether relatively high integrin mRNA levels are correlated with successful cell attachment and survival on BM, integrin mRNA levels were quantified for hES-RPE (Fig. 13) and four fRPE cultures used for seeding onto BM (Fig. 14). The integrin mRNA levels were compared to cell behavior after days 1 and 21 in organ culture. The results are reported relative to hES-RPE1 for the three hES-RPE batches and relative to a passage-3 day-5 fRPE culture for fRPE. hES-RPE1, which showed significantly higher nuclear density than hES-RPE2 and hES-RPE3 at day 1 (see Fig. 1), had higher mRNA levels of integrins α1–5 and β1 than hES-RPE2 but lower levels of α2, 4, 5, and β1 than hES-RPE3. (Integrins α1–5, and β1 are important in RPE attachment to hES-RPE.[4,20]) The integrin mRNA levels of α1–5 and β1 in hES-RPE3 were higher than those of hES-RPE2, yet the nuclear density at day 1 was similar, indicating that these mRNA integrin profiles may not be the best indicator of these cells' ability to adhere to BM initially. Long-term survival on equatorial BM also did not appear to be correlated with relatively high integrin α1–5 and β1–6 mRNA levels, because both hES-RPE2 and hES-RPE3 showed higher nuclear density than hES-RPE1 at day 21 (see Fig. 8). Bestrophin and MITF

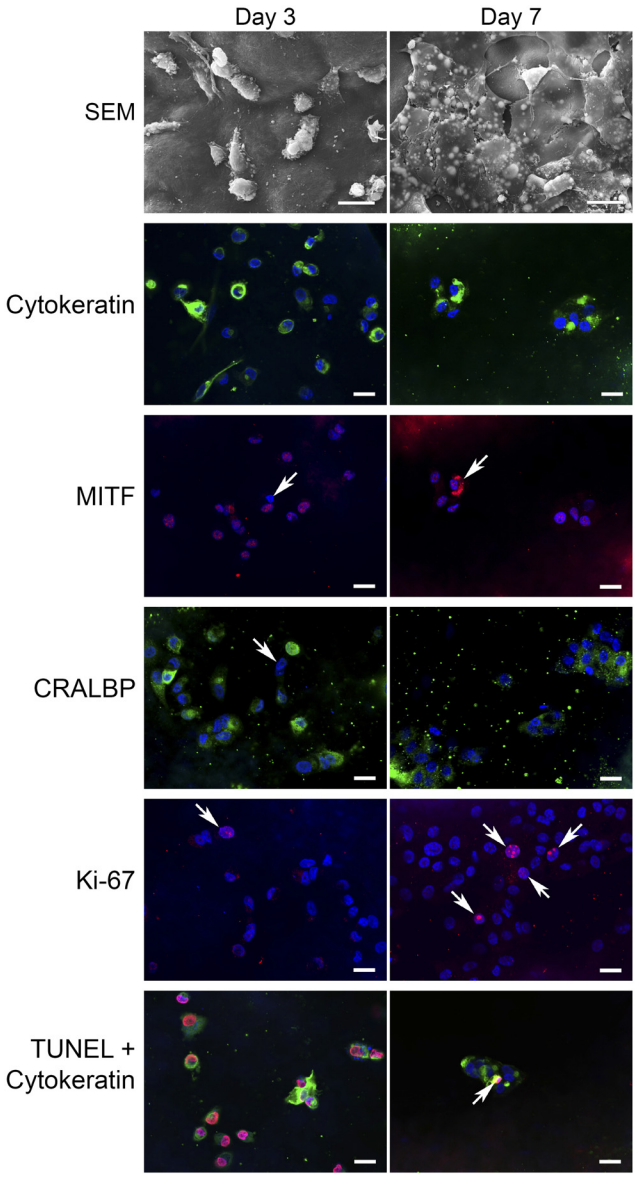

mRNA levels increased in the hES-RPE with increased time in culture and increased pigmentation.

Similarly, in fRPE cultures, relatively higher integrin mRNA levels did not appear to be correlated with cell attachment onto aged BM. In comparing integrin mRNA levels of four fRPE cultures that were seeded onto BM, two cultures with relatively high levels of α1–5 and β1 integrin mRNA (passage-4, 6 days in culture [P4, 6D] and passage-2, 4 days in culture [P2, 4D]) showed low and high nuclear densities, respectively, at day 1 (see Fig. 14). High integrin mRNA levels also did not appear to be correlated with cell survival on equatorial BM (e.g., the explant seeded with P2, 4D cells had no remaining cells at day 21). Bestrophin and MITF levels did not appear to depend on the time in culture (passage number may also affect the levels[32]).

Protein Secretion

To determine whether hES-RPE secretion of selected proteins after culture on BM is similar to that of fRPE, conditioned media above BM explants was analyzed after 21 days in organ culture, before harvesting explants for LM and SEM. Protein levels were measured for: 1) RPE media alone, 2) stem cell media alone, 3) equatorial and submacular BM explants with no previous cell seeding in stem cell or RPE media, and 4) explants with seeded cells. Equatorial and submacular BM

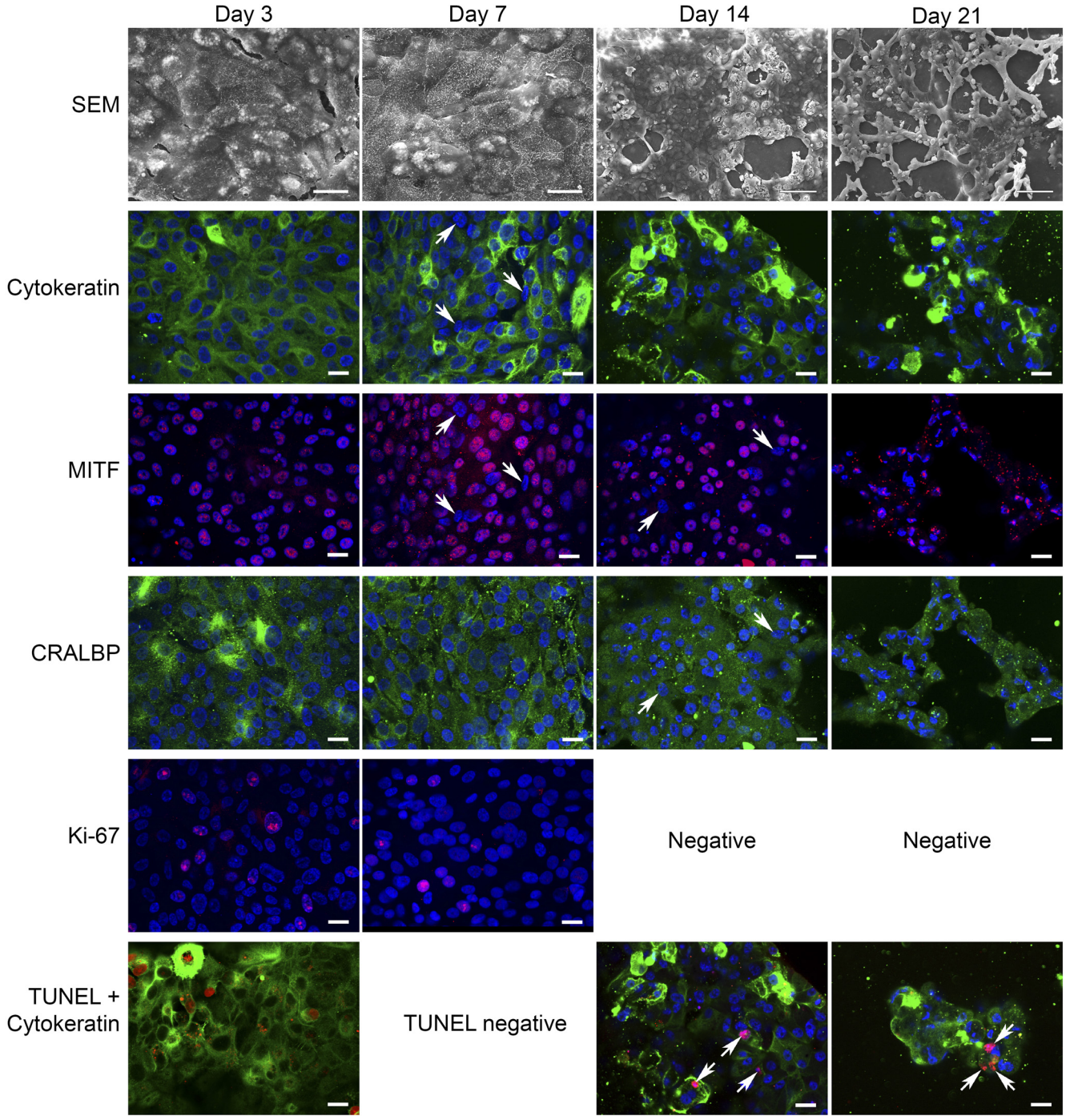

FIGURE 12.

TABLE 2. Summary of Immunostaining of hES-RPE and Fetal RPE with Time in Culture

	hES-RPE		Fetal RPE			
	Day 3	Day 7	Day 3	Day 7	Day 14	Day 21
Cytokeratin	4	4–5	5	4–5	4–5	4–5
MITF	0, 4	5	5	4–5	3–4	3–4
CRALBP	3–4	2–4	5	4–5	4	4
Ki-67	0–1	1–2	3	2–3	0–1	0–1
TUNEL	3–4	2–3	0–2	0–3	0–2	1–2

Results of hES-RPE2 and hES-RPE3 are combined and presented for day 3 and day 7 only because of limited resurfacing at later time points. Numbers are qualitative ratings (0, no label; 1, occasional labeled cell; 2, few labeled cells; 3, abundant labeled cells; 4, majority of cells labeled; and 5, all labeled).

explants incubated in stem cell or RPE media without previous cell seeding were analyzed for protein secretion to determine choroid and sclera contribution to the protein levels in conditioned media. Protein levels were corrected by subtracting the amounts detected in media alone (not exposed to explants). Protein levels (log pg/mL) associated with equatorial and submacular explants (no cell seeding) in both media are shown in Figure 15. All protein levels were above the amounts detected in media alone except for PEDF. Significant differences ($^*P < 0.05$) were noted between equatorial and submacular explants in RPE media for PEDF and equatorial and submacular explants in stem cell media for TGFβ2. Negative values are represented as 0 in Figure 15.

Protein levels determined from conditioned media harvested from paired BM explants seeded with hES-RPE2 or hES-RPE3 and explants seeded with fRPE were normalized to nuclear density (Fig. 16). Protein levels for equatorial or submacular explants seeded with hES-RPE2 or hES-RPE3 were not statistically different (Mann-Whitney rank sum test, $P > 0.05$), and the groups were combined. Protein levels of hES-RPE1 on equatorial and submacular BM explants were not shown because of the low survival of this preparation on both equatorial and submacular BM at day 21 (see Figs. 5, 8). Protein levels for explants with seeded cells were included only if the nuclear density was $>$ 2 nuclei per millimeter of BM to exclude explants where secretion was primarily from the explant. Secretion levels for TNF-α were not above choroid/sclera secretion levels for hES-RPE or fRPE on equatorial and submacular explants and, therefore, were not included in the analysis. Negative numbers (secretion from choroid/sclera higher than choroid/sclera seeded with cells) were represented as 0 in Figure 16.

On equatorial BM explants, hES-RPE protein secretion levels were above explant levels for NGF, BDNF, IGFBP3, PEDF, and TSP2, while fRPE protein secretion levels were above explant levels for BDNF, VEGF, PEDF, and TGFβ2. On submacular BM explants, hES-RPE showed protein secretion levels above explant levels for NGF, IGFBP3, PEDF, TSP2, and TGFβ2, while fRPE showed secretion above explant levels for all proteins except TSP2.

FIGURE 12. fRPE behavior on submacular human Bruch's membrane after 3, 7, 14, and 21 days in culture. Explants were immunostained for cytokeratin (FITC), MITF (rhodamine), CRALBP (FITC), Ki-67 (rhodamine), or TUNEL (rhodamine) followed by nuclear staining with the dye, TO-PRO-3 (*blue*). *Day 3*: fRPE on Bruch's membrane from a 74-year-old female with AMD (same donor as Fig. 11, *Day 3*). *SEM*: Large, flat cells almost fully resurfaced the explant. Many of the cells contain abundant small vacuoles. *Cytokeratin*: All cells showed strong cytokeratin labeling. *MITF* (same field as cytokeratin): All cells showed nuclear staining of MITF. *CRALBP*: All cells showed some degree of cytoplasmic staining for CRALBP. *Ki-67*: Several Ki-67–positive cells are present in this field. Ki-67–positive cells were fairly abundant at this time point. *TUNEL + cytokeratin*: Abundant TUNEL-positive cells were observed on this explant. Eight TUNEL-positive nuclei are in this field with one TUNEL-positive cell also showing intense cytokeratin staining. (No TO-PRO-3 staining.) *Day 7*: fRPE on Bruch's membrane from an 80-year-old female with few hard submacular drusen (same donor as Fig. 11, *Day 7*). *SEM*: fRPE almost fully resurface the explant with flat cells of varying sizes. The number of cells containing vacuoles is not as frequent as at day 3. *Cytokeratin*: The majority of cells appear be labeled for cytokeratin, although some cells appear to be labeled sparsely or unlabeled while other cells show intense staining. *Arrows*: cells with no or sparse cytokeratin label. *MITF* (same field as cytokeratin): Several MITF-negative nuclei are seen in this field. MITF-negative nuclei (*arrows* in both MITF and cytokeratin images) appear to be sparsely labeled or unlabeled for cytokeratin. *CRALBP*: All cells show cytoplasmic CRALBP label. *Ki-67*: Ki-67–positive nuclei were seen in localized areas on this explant. *TUNEL + cytokeratin*: No TUNEL-positive nuclei were detected. *Day 14*: fRPE seeded on a submacular explant of an 80-year-old female with no submacular pathology. *SEM*: fRPE were present as a partially confluent layer of cells with many defects of varying sizes. Patches of dead (not intact) cells can be seen within the monolayer. *Cytokeratin*: Most of the cells show cytokeratin staining, with some cells showing tense labeling. In some cells, the staining is faint or sparse. *MITF*: Not all nuclei stain positive for MITF. *Arrows* indicate two unlabeled nuclei that are also pointed to by *arrows* in the CRALBP image. TO-PRO-3 staining reveals several condensed nuclei. *CRALBP*: Most of the cells show some degree of CRALBP staining in the nucleus. *Arrows* point to two cells that show CRALBP labeling in the cytoplasm that are MITF-negative. *Ki-67*: No Ki-67–positive cells were observed on this explant. *TUNEL + cytokeratin*: TUNEL-positive nuclei were sparse at this time point. *Arrows* point to nuclei that are labeled. These were the only TUNEL-positive cells observed on submacular Bruch's membrane of this explant. *Day 21*: fRPE seeded on a submacular explant from an 80-year-old female with no submacular pathology (fellow eye of day 14 donor). *SEM*: Severely impaired resurfacing was observed on this explant with many cells exhibiting long lamellipodia. Mixed in with the enlarged, elongate cells are small patches of flattened cells and rounded cells. No cells were present in the center of submacular Bruch's membrane. *Cytokeratin*: Cytokeratin and TO-PRO-3 staining show the cells are not as well spread as at earlier time points with many cells showing intense cytokeratin staining with abundant condensed and misshapen nuclei. Some cells show no or sparse cytokeratin staining. *MITF*: Many of the condensed, misshapen nuclei show MITF labeling although the labeling does not appear to co-localize with TO-PRO-3 staining. Punctate cytoplasmic staining appears to be autofluorescent granules that also appear in the CRALBP image. *CRALBP* (same field as MITF image): The majority of cells stain positive for cytoplasmic CRALBP, even cells with condensed nuclei. *Ki-67*: No Ki-67–positive nuclei were observed on this explant. *TUNEL + cytokeratin*: Few TUNEL-positive nuclei (*arrows*) were observed at this time point. The nuclei indicated by the *bottom arrows* appear to be fragmented with no co-localization of the TO-PRO-3 stain. This pattern of staining was not uncommon at this time point and at the day 14 time point. In general, TUNEL-positive nuclei that were not counterstained with TO-PRO-3 were very condensed or fragmented. Scale bar: Days 14 and 21, SEM images 100 μm; for remaining SEM and confocal images 20 μm.

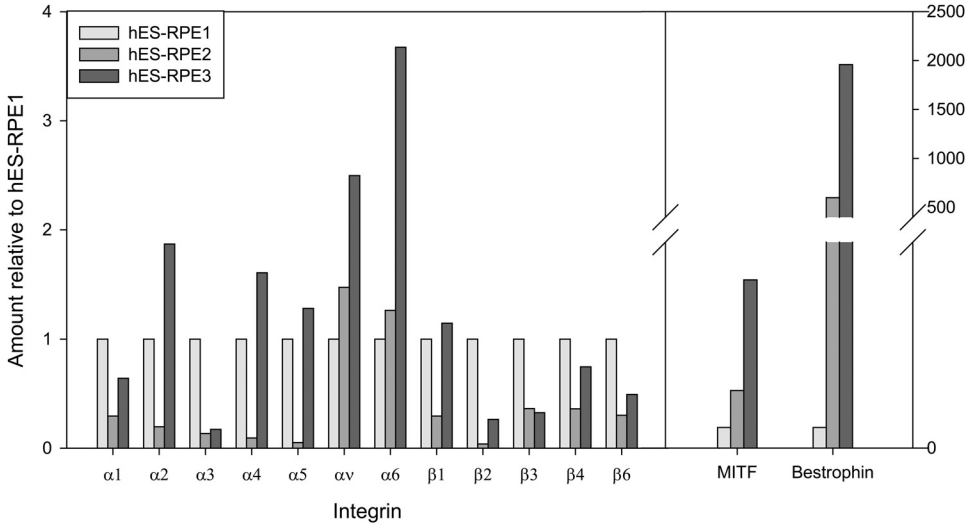

FIGURE 13. Comparison of relative amounts of integrin, bestrophin, and MITF mRNA levels among hES-RPE batches before seeding on Bruch's membrane. mRNA levels are expressed relative to levels in hES-RPE1.

Data for secretion levels of explant preparations for each protein were analyzed for significant differences by Kruskal-Wallis one-way ANOVA on ranks. When differences in the median values were statistically significant, all pairwise multiple comparison procedures (Dunn's method) testing was performed. The results, shown in Figure 16, indicate where differences in secretion levels were statistically significant between pairs ($^*P < 0.05$) for the remaining seven proteins. The protein secretion profiles we compared were: (1) fRPE on equatorial versus submacular BM explants, (2) hES-RPE on equatorial versus submacular explants, (3) fRPE versus hES-RPE on equatorial explants, and (4) fRPE versus hES-RPE on submacular explants. For explants seeded with fRPE, secretion from cells on submacular explants was higher than from cells on equatorial explants for NGF, IGFBP3, and PDGF. For explants seeded with hES-RPE, secretion from cells on submacular explants was significantly higher than from cells on equatorial explants for TGFβ2. On equatorial explants, hES-RPE secretion was significantly higher than fRPE secretion for NGF and TSP2. On submacular explants, hES-RPE secretion was significantly higher than fRPE secretion for TSP2, and fRPE secretion was significantly higher than hES-RPE secretion for BDNF, VEGF, and PDGF (see Fig. 12). PEDF secretion was similar for hES-RPE and fRPE on submacular and equatorial BM explants.

DISCUSSION

In previous studies, fRPE showed limited survival on aged and AMD submacular BM at day 14 in organ culture with a decline in nuclear density from day 1 to day 14.[13] The data reported here are consistent with these results and show a continuous decline in fRPE resurfacing on aged and AMD submacular BM explants between days 3 and 21 in organ culture. hES-RPE also show impaired survival on aged and AMD submacular BM. However, while fRPE are able to resurface submacular BM to a high degree after 3 days in culture, the initial attachment and

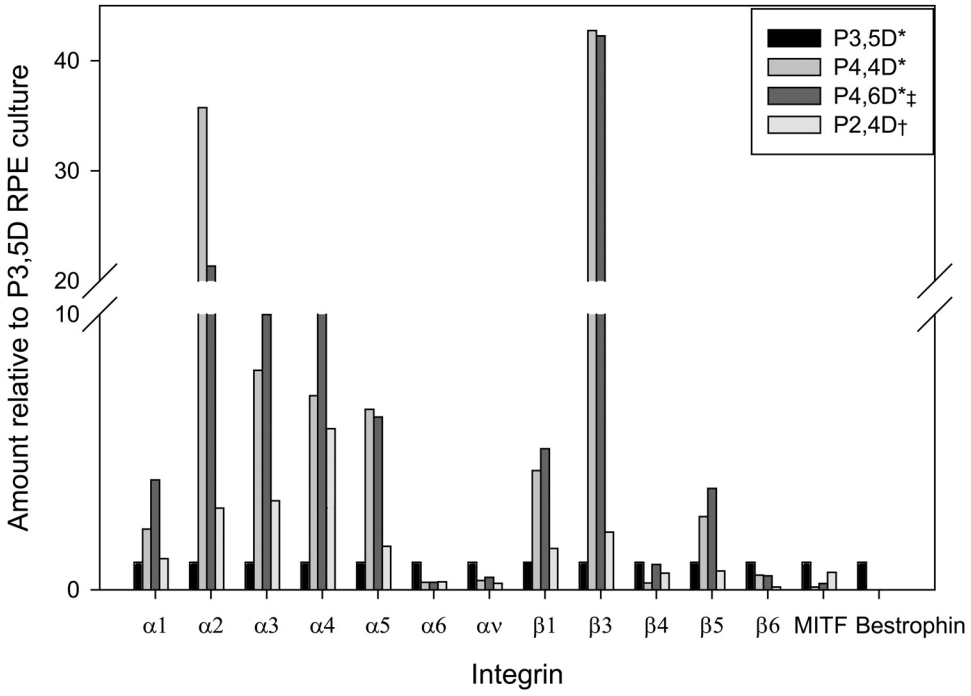

FIGURE 14. Comparison of relative amounts of integrin, bestrophin, and MITF mRNA levels in four fRPE cell cultures (*P*, passage number; *D*, days in culture) before seeding onto aged human equatorial Bruch's membrane. Integrin mRNA levels are relative to levels in P3, 5D fRPE. *Cultures from the same primary culture. †Of the four cultures, the culture showing highest nuclear density at day 1 on equatorial Bruch's membrane. ‡Of the four cultures, the culture showing the lowest nuclear density at day 1 on equatorial Bruch's membrane.

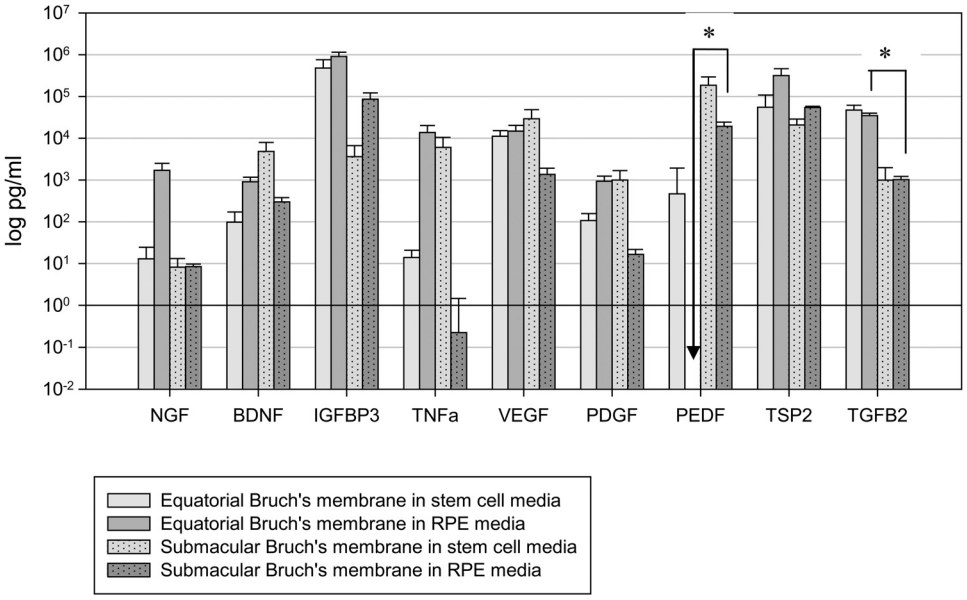

FIGURE 15. Contribution of the Bruch's membrane explant (choroid and sclera) to protein secretion (no fRPE or hES-RPE seeded). Contribution of protein secretion into the media from equatorial ($N = 4$) or submacular ($N = 5$) explants was determined after incubation for 21 days in stem cell media or RPE media. Secretion levels were corrected for levels in media only and are expressed as mean log pg/mL (error bars = SEM). Secretion was significantly different between pairs noted with an asterisk ($P < 0.05$) for PEDF and TGFβ2.

survival of hES-RPE appears to be severely impaired. Further decline in hES-RPE cell number with time is indicated by the large number of TUNEL-positive cells with no or few proliferating cells (Ki-67–positive) at day 3 and continued presence of TUNEL-positive hES-RPE cells at day 7. FRPE appeared to be relatively healthy up to day 7 in culture and demonstrated proliferating cells, well-formed nuclei (indicated by TO-PRO-3 staining), and a paucity of TUNEL-positive cells. By day 14, SEM showed impaired resurfacing by fRPE, indicating a significant amount of cell death between 7 and 14 days, which appears to continue up to 21 days in culture, the longest time point in this study. The poor health of the cells is indicated by the presence of dying or dead cells on BM as visualized by SEM and the abundance of condensed, fragmented, and misshapen nuclei. We have shown that fRPE survival on aged submacular human BM can be enhanced greatly if the inner collagenous layer is resurfaced by an appropriate extracellular matrix.[33] Nuclear densities in the latter study were increased by approximately twofold after submacular BM resurfacing in aged Caucasian donors. It is therefore possible for cells to survive on aged submacular human BM after surface treatment of BM, and the cell death observed in the present study represents a toxic effect of BM on the cells and not an organ culture artifact.[33]

An epithelial cell marker (cytokeratin) and two RPE markers (MITF, an RPE transcription factor, and the visual cycle protein CRALBP) were used to determine the ability of hES-RPE and fRPE to maintain these RPE markers with time in culture after seeding onto submacular BM. hES-RPE and fRPE were able to maintain the epithelial marker and strongly expressed cytokeratin in cells with normal and abnormal nuclear morphology. Upregulation of cytoskeletal proteins such as cytokeratin has been shown previously to be associated with dedifferentiated RPE.[34] The loss of CRALBP and MITF in hES-RPE may be related to cell health at day 3 because many cells appeared to be dying. The majority of fRPE expressed the three markers and appeared capable of maintaining the markers at later time points, even when cell health declined. The loss of markers in some cells at later time points did not specifically appear to be related to cell health, because some cells with well-formed nuclei did not express MITF or CRALBP. One explanation is

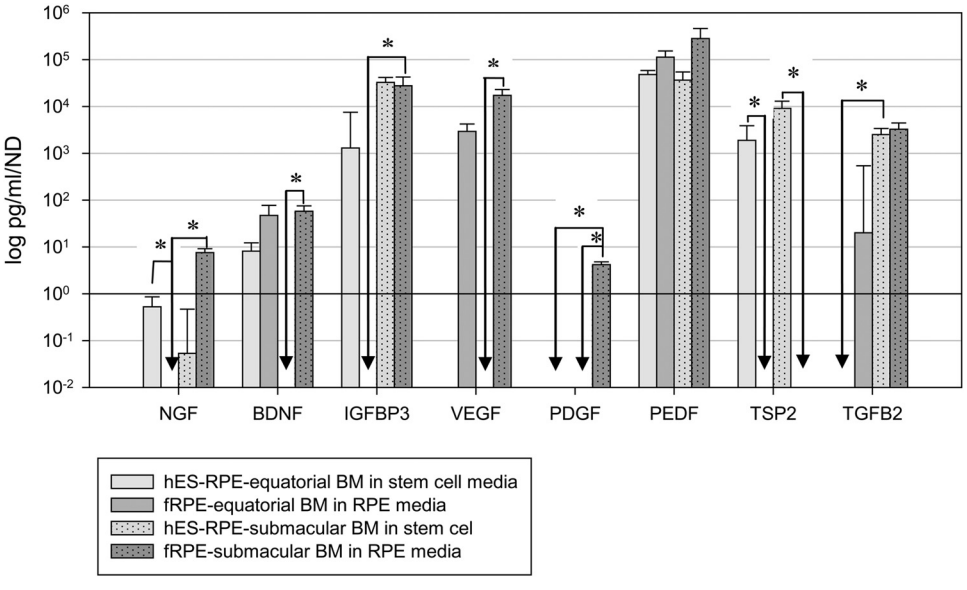

FIGURE 16. hES-RPE and fRPE secretion on equatorial and submacular Bruch's membrane explants. Protein levels have been corrected for contribution from the explant (Fig. 15) and are normalized to nuclear density. Pairwise comparisons between explant preparations were performed for each protein. Significant differences between pairs are indicated (*$P < 0.05$).

that the cells were labeled, but the labeling intensity was not high enough to detect over BM autofluorescence. Alternatively, the cells could have undergone dedifferentiation, because suppression of MITF and CRALBP is associated with dedifferentiation (loss of mature RPE features).[34–37] Nuclear staining of CRALBP has been shown previously,[38,39] although the confocal study by Huang et al.[39] attributed nuclear labeling to an artifact from *z*-stack projection. Because the images obtained in this study were single *z*-sections, this type of artifact would not be present.

The nuclear density of hES-RPE1 seeded on submacular BM explants was significantly lower than that of fRPE on fellow eye submacular explants at day 21. Although the more pigmented batches of hES-RPE exhibited nuclear densities at day 21 that were statistically similar to those of fRPE on fellow eye explants, hES-RPE generally showed worse morphology with membrane holes, membrane blebs, loss of cytoplasm, and vacuole formation was observed more frequently than that seen with fRPE. Study of hES-RPE2 and hES-RPE3 behavior at intermediate time points showed impaired resurfacing and poor cell health compared to fRPE cultured for the same period on fellow eye explants. We interpret these findings to mean that all the batches of hES-RPE show a trend toward poorer cell survival on aged human submacular BM explants compared to fRPE.

Although fRPE exhibited relatively better survival on aged and AMD BM than hES-RPE, survival of all cells on aged and AMD submacular BM was impaired, with mean nuclear densities (approximately 13 nuclei/mm on BM at day 21) well below that reported for fRPE cells on culture dishes (approximately 45 nuclei/mm at day 14), and below that reported for in situ RPE in aged donors (approximately 30 nuclei/mm on BM for donors 70 years of age and above).[13] The poor survival of these robust cells may indicate that aged/AMD BM will not support healthy RPE cells and that some method must be developed to prevent cell death on aged/AMD BM for RPE transplants to be successful in aged patients. This notion is consistent with the long-term results of RPE transplantation in patients with AMD (both atrophic and neovascular forms), which typically has resulted in limited visual recovery regardless of the type of cell transplanted (e.g., autologous or allogeneic, adult or fRPE) and regardless of whether the cells are transplanted with or without choroid (see review by da Cruz et al.[40]). Tezel et al.[41,42] reported impaired survival on peripheral and equatorial inner collagenous layer of aged donors (pathology unknown) by cultured adult RPE (at day 21) or fRPE (at day 17) with no or few cells remaining. Compared to the results reported by Tezel at al., we observed relatively better survival on equatorial BM explants by both fRPE and hES-RPE2 and hES-RPE3. The differences in survival may be related to differences in experimental technique (e.g., higher initial seeding density in the present study), different methods of preparing BM to expose the inner collagenous layer (our methods are mechanical with no exposure to chemicals), and differences in fRPE cultures (e.g., passage number or time in culture).

The aim of this study was to determine whether hES-RPE could be a considered as a candidate for cell transplantation in AMD patients. The most relevant surface on which to assess cell survival in this context is aged submacular human BM. However, to compare fRPE and hES-RPE preparations within the same donor eye, we compared attachment on equatorial BM. (There is not enough submacular BM tissue to permit assay of the two cell types on a single specimen with our current techniques.) FRPE, hES-RPE2, and hES-RPE3 behavior on equatorial explants differed from that seen for fRPE behavior on aged submacular BM. On submacular BM, we observed a decline in fRPE cell numbers with time in culture while on equatorial explants, there was no significant decline in the nuclear density from day 1 to day 21, indicating that after day 1, no further cell death occurred or cell proliferation occurred at a rate similar to cell death. Tezel et al. showed approximately 0.2% of fRPE seeded on the "peripheral" inner collagenous layer were positive for apoptosis at 24 hours, and no cells tested positive for proliferation. (There was a decline in cell number from 6 to 24 hours.[10]) The results from the present study demonstrate that fRPE can proliferate on submacular inner collagenous layer, so it is possible that proliferation may play an important role in maintaining nuclear density at later times in culture regardless of the BM location.

The poor attachment of all hES-RPE preparations to equatorial BM at day 1 may be related to the fact that the cells were from frozen stock and required time to recover after thaw. The differences in initial attachment of hES-RPE1 versus hES-RPE2 and hES-RPE3 may be related to: 1) their time in culture before harvest and/or 2) differences that may exist between cells harvested from cultures with different media (hES-RPE1 cultures were in a different medium than hES-RPE2 and hES-RPE3). These factors may be more important than integrin mRNA expression in influencing cell attachment at day 1. For example, although hES-RPE3 exhibited increased integrin mRNA expression compared to hES-RPE2 for all integrins tested (except $\beta 3$; see Fig. 13), hES-RPE3 did not exhibit greater attachment to BM at day 1 in organ culture compared to hES-RPE2. Initial integrin mRNA expression also did not appear to correlate with long-term RPE survival on BM because hES-RPE2 and hES-RPE3 survival were identical on equatorial and submacular BM. A limitation of the present study is that neither the integrin protein levels nor the presence of integrins on the cell surface was determined. However, these integrin studies were performed solely to determine whether an "integrin mRNA profile" could be used as a selection criterion for hES-RPE that would predict the capacity to survive on aged BM. Previous studies showed that integrins $\alpha 1$–5 are important for cultured adult RPE adhesion to aged BM exhibiting no signs of AMD.[20] The results presented here, using fRPE and hES-RPE on aged and AMD BM, show that factors other than or in addition to integrin mRNA levels are important in initial attachment and long-term survival of these cells on aged and AMD BM.

Subretinal injection of the batches of hES-RPE used in this study induced similar degrees of photoreceptor survival and visual acuity improvement in RCS rats.[8] Our studies indicate that hES-RPE1 behavior on equatorial explants from aged and AMD BM is significantly different from that of hES-RPE2 and hES-RPE3. In contrast to the nuclear density of the more pigmented hES-RPE2 and hES-RPE3 and fRPE cells, hES-RPE1 nuclear density showed a decline from day 1 to day 21 on equatorial BM explants. Gene profiling of the three batches of hES-RPE showed that hES-RPE1 cluster closer to fRPE than hES-RPE2 and hES-RPE3.[8] One might expect hES-RPE1 behavior to resemble more closely that of fRPE compared to hES-RPE2 and hES-RPE3. However, hES-RPE2 and hES-RPE3 expressed higher levels of RPE-specific genes than hES-RPE1.[8] We do not know if this difference accounts for the relatively better survival of the more pigmented hES-RPE2 and hES-RPE3 on equatorial BM versus that of hES-RPE1. We note, however, that the three batches showed very similar behavior on aged submacular human BM.

We found that the equatorial inner collagenous layer can show aging changes similar to those seen in the submacular inner collagenous layer in aged and AMD donors, and the changes evident by toluidine blue staining of tissue sections are highly variable, even within the same donor eye. The poor RPE survival on the equatorial inner collagenous layer reported here and by Tezel et al.[42] indicate that age-related changes affecting cell survival on the inner collagenous layer may not be limited to the submacular region. Therefore, BM changes

affecting RPE survival in AMD patients may not be limited to submacular BM.

Rescued photoreceptors are present some distance away from transplanted RPE cells,[8,23,43] which indicates that trophic factors secreted by transplanted cells may be an important component of their salutary effect on host retina. Secretion of neuroprotective factors may play a role in the prevention of retinal degeneration after subretinal transplantation of non-RPE cells.[23,25,43] During the time required for transplanted hES-RPE and fRPE to differentiate and become fully functional RPE on aged and AMD BM, secretion of neuroprotective factors may help to prevent further retinal degeneration. Neurotrophin secretion may occur even if the RPE cells do not differentiate fully. In the present study, submacular BM explants exhibiting the best cell survival did not feature hES-RPE or fRPE with the morphology of mature RPE (i.e., columnar cells, apical-basal orientation, pigmentation, and well developed apical processes). To determine whether hES-RPE secrete neurotrophic factors and other proteins that fRPE secrete in detectable amounts after seeding on BM, we compared proteins in conditioned media from hES-RPE and fRPE seeded on equatorial and submacular BM explants at day 21 in organ culture. To determine which proteins to assay, we analyzed conditioned media from 21-day fRPE cultures. All conditioned media analyzed include bovine serum (which contains growth factors); RPE media also contained bFGF. Media alone did not exhibit high levels of any of the proteins tested, which may be due in part to the specificity of the assay for human proteins (data not shown). Included among the proteins analyzed were those shown to have retina-preserving properties in vivo (e.g., NGF,[44] BDNF,[45–48] TNF-α,[47] PEDF,[49,50]) and IGFBP3, VEGF, TSP2, and TGFβ2, which were present in detectable amounts in RPE-conditioned media from fRPE cultures.

To identify protein secretion from seeded cells, we determined levels of the aforementioned proteins in equatorial and submacular BM explants that had not been seeded with cells. Levels above those in media alone were found for all proteins tested in both equatorial and submacular explants (Fig. 15). Although there are no published studies on secretion of human BM explants (which consist of sclera, choroid, and BM), secretion of VEGF, TNF-α, and PDGF-β has been attributed to rat choroid explants[51]; VEGF secretion has been detected in cultured choroidal endothelial cells.[52] Growth factor secretion was similar in both equatorial and submacular BM explants, regardless of media, except for higher PEDF levels in submacular versus equatorial explants in RPE media and higher TGFβ2 levels from equatorial versus submacular explants in stem cell media. Secretion attributed to RPE/hES-RPE cells at day 21 after seeding on BM explants was seen for some proteins. Secretion of the two cell types was similar on equatorial explants for all proteins tested except for NGF and TSP2, which were higher in hES-RPE–conditioned media. More differences were noted between cell types on submacular explants, where hES-RPE secretion was higher for TSP2, and fRPE secretion was significantly higher for BDNF, VEGF, and PDGF. The three proteins secreted in the highest amounts by fRPE on submacular explants were IGFBP3, VEGF, and PEDF. hES-RPE did not secrete VEGF above levels measured for submacular BM explants without RPE. A study by Ohno-Matsui et al.[53] showed that VEGF secretion by RPE depends on the degree of differentiation; there was a more than threefold difference in VEGF secretion between differentiated cells (grown on laminin) and undifferentiated cells (grown on plastic). The poorer viability of hES-RPE on BM could contribute to lack of VEGF secretion on the explants, because VEGF mRNA levels were high in hES-RPE3 before seeding on BM, and low density cultures of hES-RPE3 on tissue culture–treated plastic did show detectable VEGF in conditioned media harvested at day 21 (data not shown). The lack of VEGF secretion by hES-RPE after seeding on aged and AMD BM may be significant, because RPE secretion of VEGF is important in the maintenance of choriocapillaris health and is required for maintenance of choriocapillaris fenestration.[54–57] PEDF and IGFBP3, a protein implicated in retinal vascular repair and protection from damage after oxygen-induced vessel loss,[58] were similarly secreted by both hES-RPE and fRPE on submacular explants. Lastly, hES-RPE secreted significantly higher amounts of TSP2 than fRPE on both equatorial and submacular explants. TSP2 has antiangiogenic properties (e.g., can inhibit pro-angiogenic properties of VEGF).[59–61]

Whether differences in protein secretion of hES-RPE versus fRPE cultured on BM will affect the maintenance of choriocapillaris function, retina preservation, and other functions influenced by RPE is unknown. For example, of the neurotrophins tested, BDNF was the only protein showing differences in secretion on submacular explants with hES-RPE showing significantly less protein levels than fRPE. It is unclear that low BDNF levels will interfere with cell-mediated photoreceptor rescue as other neurotrophins (e.g., PEDF) were present in relatively high levels. Neurotrophic factors may not be interchangeable in their ability to prevent retinal degeneration as synergistic effects existing between factors and pathways of rescue, and target cells and their receptors may vary. For example, two receptor families (FGF receptor and TRK neutrophin receptors) and their respective ligands (including bFGF, BDNF, and NGF) can provide neuroprotection. More than one neurotrophic factor can activate the same receptor, and the target cell could be Müller cells rather than photoreceptors (reviewed by Chaum[62]). One limitation of the present study is that differences in media used for organ culture of the two cell types could possibly affect cell secretion. Studies by Rosenthal et al.[63] showed that bFGF can increase VEGF secretion, although the amount used in the Rosenthal study was 10 times higher than the amount present in RPE media, and VEGF secretion was similar on BM explants cultured in the two media. Animal studies indicate the potential of relatively healthy hES-RPE to support visual acuity over long survival times.[8,16] The poor viability of hES-RPE on aged and AMD BM may lead to differences in protein secretion from that observed in these animal studies.

Cells whose behavior we have tested using this BM paradigm include fRPE and aged adult RPE,[4,12,13,20,64] iris pigment epithelium,[22] and human adult stem cells (unpublished studies). Of the cells tested on BM, hES-RPE with $>$ 50% of cultured cells showing pigmentation (i.e., hES-RPE2 and hES-RPE3) and fRPE show the best ability to survive to some extent on aged/AMD submacular human BM. The results of this study combined with the results of in vivo studies showing hES-RPE can prevent photoreceptor degeneration in rodent models and the safety of the cells after subretinal injection[8,14,16] suggest that hES-RPE might be considered as an alternative to fRPE for cell replacement therapy in AMD patients. The poor survival of hES-RPE and fRPE on AMD explants, however, indicates that methods to improve cell survival on aged/diseased BM should be included in the development of cell-based therapy for AMD patients.

Acknowledgments

The authors thank Lucy Vilner for technical assistance with hES-RPE culture.

References

1. Binder S, Stanzel BV, Krebs I, Glittenberg C. Transplantation of the RPE in AMD. *Prog Retin Eye Res.* 2007;26:516–554.

2. Del Priore LV, Geng L, Tezel TH, Kaplan HJ. Extracellular matrix ligands promote RPE attachment to inner Bruch's membrane. *Curr Eye Res.* 2002;25:79–89.
3. Ho TC, Del Priore LV. Reattachment of cultured human retinal pigment epithelium to extracellular matrix and human Bruch's membrane. *Invest Ophthalmol Vis Sci.* 1997;38:1110–1118.
4. Zarbin MA. Analysis of retinal pigment epithelium integrin expression and adhesion to aged submacular human Bruch's membrane. *Trans Am Ophthalmol Soc.* 2003;101:499–520.
5. Boulton M, Róanowska M, Wess T. Ageing of the retinal pigment epithelium: implications for transplantation. *Graefes Arch Clin Exp Ophthalmol.* 2004;242:76–84.
6. Hageman GS, Anderson DH, Johnson LV, et al. A common haplotype in the complement regulatory gene factor H (HF1/CFH) predisposes individuals to age-related macular degeneration. *Proc Natl Acad Sci U S A.* 2005;102:7227–7232.
7. Gullapalli VK, Sugino IK, Zarbin MA. Muller cells and the retinal pigment epithelium. In: Albert CM, Miller JW, Azar DT, Blodi BA, eds. *Albert & Jakobiec's Principles & Practice of Ophthalmology.* Philadelphia: Saunders; 2008.
8. Lu B, Malcuit C, Wang S, et al. Long-term safety and function of RPE from human embryonic stem cells in preclinical models of macular degeneration. *Stem Cells.* 2009;27:2126–2135.
9. Klimanskaya I, Hipp J, Rezai KA, West M, Atala A, Lanza R. Derivation and comparative assessment of retinal pigment epithelium from human embryonic stem cells using transcriptomics. *Cloning Stem Cells.* 2004;6:217–245.
10. Klimanskaya I, Chung Y, Becker S, Lu SJ, Lanza R. Human embryonic stem cell lines derived from single blastomeres. *Nature.* 2006;444:481–485.
11. Klimanskaya I, Rosenthal N, Lanza R. Derive and conquer: sourcing and differentiating stem cells for therapeutic applications. *Nat Rev Drug Discov.* 2008;7:131–142.
12. Castellarin AA, Sugino IK, Vargas JA, Parolini B, Lui GM, Zarbin MA. In vitro transplantation of fetal human retinal pigment epithelial cells onto human cadaver Bruch's membrane. *Exp Eye Res.* 1998; 66:49–67.
13. Gullapalli VK, Sugino IK, Van Patten Y, Shah S, Zarbin MA. Impaired RPE survival on aged submacular human Bruch's membrane. *Exp Eye Res.* 2005;80:235–248.
14. Vugler A, Carr AJ, Lawrence J, et al. Elucidating the phenomenon of HESC-derived RPE: anatomy of cell genesis, expansion and retinal transplantation. *Exp Neurol.* 2008;214:347–361.
15. Carr AJ, Vugler A, Lawrence J, et al. Molecular characterization and functional analysis of phagocytosis by human embryonic stem cell-derived RPE cells using a novel human retinal assay. *Mol Vis.* 2009;15:283–295.
16. Lund RD, Wang S, Klimanskaya I, et al. human embryonic stem cell-derived cells rescue visual function in dystrophic RCS rats. *Cloning Stem Cells.* 2006;8:189–199.
17. Idelson M, Alper R, Obolensky A, et al. Directed differentiation of human embryonic stem cells into functional retinal pigment epithelium cells. *Cell Stem Cell.* 2009;5:396–408.
18. Gullapalli VK, Khodair MA, Wang H, Sugino IK, Madreperla S, Zarbin MA. Retinal pigment epithelium and photoreceptor transplantation frontiers. In: Ryan SJ, ed. *Retina.* 4th ed. Vol III. Philadelphia: Mosby, Inc.; 2006:2597–2613.
19. Afshari FT, Fawcett JW. Improving RPE adhesion to Bruch's membrane. *Eye (Lond).* 2009;23:1890–1893.
20. Gullapalli VK, Sugino IK, Zarbin MA. Culture-induced increase in alpha integrin subunit expression in retinal pigment epithelium is important for improved resurfacing of aged human Bruch's membrane. *Exp Eye Res.* 2008;86:189–200.
21. Proulx S, Guerin SL, Salesse C. Effect of quiescence on integrin alpha5beta1 expression in human retinal pigment epithelium. *Mol Vis.* 2003;9:473–481.
22. Itaya H, Gullapalli V, Sugino IK, Tamai M, Zarbin MA. Iris pigment epithelium attachment to aged submacular human Bruch's membrane. *Invest Ophthalmol Vis Sci.* 2004;45:4520–4528.
23. Wang S, Lu B, Wood P, Lund RD. Grafting of ARPE-19 and Schwann cells to the subretinal space in RCS rats. *Invest Ophthalmol Visual Sci.* 2005;46:2552–2560.
24. Lawrence JM, Sauve Y, Keegan DJ, et al. Schwann cell grafting into the retina of the dystrophic RCS rat limits functional deterioration. *Invest Ophthalmol Vis Sci.* 2000;41:518–528.
25. Lawrence JM, Keegan DJ, Muir EM, et al. Transplantation of Schwann cell line clones secreting GDNF or BDNF into the retinas of dystrophic Royal College of Surgeons rats. *Invest Ophthalmol Vis Sci.* 2004;45:267–274.
26. Pinilla I, Cuenca N, Martinez-Navarrete G, Lund RD, Sauve Y. Intraretinal processing following photoreceptor rescue by non-retinal cells. *Vision Res.* 2009;49:2067–2077.
27. Klimanskaya I, Chung Y, Becker S, Lu SJ, Lanza R. Derivation of human embryonic stem cells from single blastomeres. *Nat Protoc.* 2007;2:1963–1972.
28. Klimanskaya I. Retinal pigment epithelium. *Methods Enzymol.* 2006;418:169–194.
29. Gullapalli VK, Sugino IK, Van Patten Y, Shah S, Zarbin MA. Retinal pigment epithelium resurfacing of aged submacular human Bruch's membrane. *Trans Am Ophthalmol Soc.* 2004;102:123–137.
30. Song MK, Lui GM. Propagation of fetal human RPE cells: preservation of original culture morphology after serial passage. *J Cell Physiol.* 1990;143:196–203.
31. Nasir MA, Sugino IK, Zarbin MA. Decreased choriocapillaris perfusion following surgical excision of choroidal neovascular membranes in age-related macular degeneration. *Br J Ophthalmol.* 1997;81:481–489.
32. Rak DJ, Hardy KM, Jaffe GJ, McKay BS. Ca++-switch induction of RPE differentiation. *Exp Eye Res.* 2006;82:648–656.
33. Sugino IK, Gullapalli VK, Sun S, et al. Cell-deposited matrix improves retinal pigment epithelium survival on aged submacular human Bruch's membrane. *Invest Ophthalmol Vis Sci.* 2011;52: 1345–1358.
34. Alge CS, Suppmann S, Priglinger SG, et al. Comparative proteome analysis of native differentiated and cultured dedifferentiated human RPE cells. *Invest Ophthalmol Vis Sci.* 2003;44:3629–3641.
35. Liu Y, Xin Y, Ye F, et al. Taz-tead1 links cell-cell contact to zeb1 expression, proliferation, and dedifferentiation in retinal pigment epithelial cells. *Invest Ophthalmol Vis Sci.* 2010;51:3372–3378.
36. Liu Y, Ye F, Li Q, et al. Zeb1 represses Mitf and regulates pigment synthesis, cell proliferation and epithelial morphology. *Invest Ophthalmol Vis Sci.* 2009;50:5080–5088.
37. Iwakiri R, Kobayashi K, Okinami S, Kobayashi H. Suppression of Mitf by small interfering RNA induces dedifferentiation of chick embryonic retinal pigment epithelium. *Exp Eye Res.* 2005; 81:15–21.
38. Anderson DH, Neitz J, Saari JC, et al. Retinoid-binding proteins in cone-dominant retinas. *Invest Ophthalmol Vis Sci.* 1986;27:1015–1026.
39. Huang J, Possin DE, Saari JC. Localizations of visual cycle components in retinal pigment epithelium. *Mol Vis.* 2009;15:223–234.
40. da Cruz L, Chen FK, Ahmado A, Greenwood J, Coffey P. RPE transplantation and its role in retinal disease. *Prog Retin Eye Res.* 2007;26:598–635.
41. Tezel TH, Kaplan HJ, Del Priore LV. Fate of human retinal pigment epithelial cells seeded onto layers of human Bruch's membrane. *Invest Ophthalmol Vis Sci.* 1999;40:467–476.
42. Tezel TH, Del Priore LV, Kaplan HJ. Reengineering of aged Bruch's membrane to enhance retinal pigment epithelium repopulation. *Invest Ophthalmol Vis Sci.* 2004;45:3337–3348.
43. Lund RD, Wang S, Lu B, et al. Cells isolated from umbilical cord tissue rescue photoreceptors and visual functions in a rodent model of retinal disease. *Stem Cells.* 2007;25:602–611.
44. Sun X, Xu X, Wang F, et al. Effects of nerve growth factor for retinal cell survival in experimental retinal detachment. *Curr Eye Res.* 2007;32:765–772.
45. Lewis GP, Linberg KA, Geller SF, Guérin CJ, Fisher SK. Effects of the neurotrophin brain-derived neurotrophic factor in an experimental model of retinal detachment. *Invest Ophthalmol Vis Sci.* 1999;40:1530–1544.
46. Paskowitz DM, Donohue-Rolfe KM, Yang H, et al. Neurotrophic factors minimize the retinal toxicity of verteporfin photodynamic therapy. *Invest Ophthalmol Vis Sci.* 2007;48:430–437.

47. LaVail MM, Unoki K, Yasumura D, Matthes MT, Yancopoulos GD, Steinberg RH. Multiple growth factors, cytokines, and neurotrophins rescue photoreceptors from the damaging effects of constant light. *Proc Natl Acad Sci U S A.* 1992;89:11249–11253.
48. Gauthier R, Joly S, Pernet V, Lachapelle P, Di Polo A. Brain-derived neurotrophic factor gene delivery to Müller glia preserves structure and function of light-damaged photoreceptors. *Invest Ophthalmol Vis Sci.* 2005;46:3383–3392.
49. Cao W, Tombran-Tink J, Elias R, Sezate S, Mrazek D, McGinnis JF. In vivo protection of photoreceptors from light damage by pigment epithelium-derived factor. *Invest Ophthalmol Vis Sci.* 2001; 42:1646–1652.
50. Imai D, Yoneya S, Gehlbach PL, Wei LL, Mori K. Intraocular gene transfer of pigment epithelium-derived factor rescues photoreceptors from light-induced cell death. *J Cell Physiol.* 2005;202:570–578.
51. Kobayashi S, Suzuki M, Tsuneki H, Nagai R, Horiuchi S, Hagino N. Overproduction of N(epsilon)-(carboxymethyl)lysine-induced neovascularization in cultured choroidal explant of streptozotocin-diabetic rat. *Biol Pharm Bull.* 2004;27:1565–1571.
52. Hoffmann S, Friedrichs U, Eichler W, Rosenthal A, Wiedemann P. Advanced glycation end products induce choroidal endothelial cell proliferation, matrix metalloproteinase-2 and VEGF upregulation in vitro. *Graefes Arch Clin Exp Ophthalmol.* 2002;240:996–1002.
53. Ohno-Matsui K, Morita I, Tombran-Tink J, et al. Novel mechanism for age-related macular degeneration: an equilibrium shift between the angiogenesis factors VEGF and PEDF. *J Cell Physiol.* 2001;189: 323–333.
54. Saint-Geniez M, Maldonado AE, D'Amore PA. VEGF expression and receptor activation in the choroid during development and in the adult. *Invest Ophthalmol Vis Sci.* 2006;47:3135–3142.
55. Blaauwgeers HG, Holtkamp GM, Rutten H, et al. Polarized vascular endothelial growth factor secretion by human retinal pigment epithelium and localization of vascular endothelial growth factor receptors on the inner choriocapillaris. Evidence for a trophic paracrine relation. *Am J Pathol.* 1999;155:421–428.
56. Saint-Geniez M, Kurihara T, Sekiyama E, Maldonado AE, D'Amore PA. An essential role for RPE-derived soluble VEGF in the maintenance of the choriocapillaris. *Proc Natl Acad Sci U S A.* 2009;106: 18751–18756.
57. Shimomura Y, Hirata A, Ishikawa S, Okinami S. Changes in choriocapillaris fenestration of rat eyes after intravitreal bevacizumab injection. *Graefes Arch Clin Exp Ophthalmol.* 2009;247:1089–1094.
58. Chang KH, Chan-Ling T, McFarland EL, et al. IGF binding protein-3 regulates hematopoietic stem cell and endothelial precursor cell function during vascular development. *Proc Natl Acad Sci U S A.* 2007;104:10595–10600.
59. Noh YH, Matsuda K, Hong YK, et al. An N-terminal 80 kDa recombinant fragment of human thrombospondin-2 inhibits vascular endothelial growth factor induced endothelial cell migration in vitro and tumor growth and angiogenesis in vivo. *J Invest Dermatol.* 2003;121:1536–1543.
60. Streit M, Riccardi L, Velasco P, et al. Thrombospondin-2: a potent endogenous inhibitor of tumor growth and angiogenesis. *Proc Natl Acad Sci U S A.* 1999;96:14888–14893.
61. Bornstein P. Thrombospondins function as regulators of angiogenesis. *J Cell Commun Signal.* 2009.
62. Chaum E. Retinal neuroprotection by growth factors: a mechanistic perspective. *J Cell Biochem.* 2003;88:57–75.
63. Rosenthal R, Heimann H, Agostini H, Martin G, Hansen LL, Strauss O. Ca2+ channels in retinal pigment epithelial cells regulate vascular endothelial growth factor secretion rates in health and disease. *Mol Vis.* 2007;13:443–456.
64. Tsukahara I, Ninomiya S, Castellarin A, Yagi F, Sugino IK, Zarbin MA. Early attachment of uncultured retinal pigment epithelium from aged donors onto Bruch's membrane explants. *Exp Eye Res.* 2002;74:255–266.